Artemisinin induces doxorubicin resistance in human colon cancer cells via calcium-dependent activation of HIF-1α and P-glycoprotein overexpression

Riganti C, Doublier S, Viarisio D, Miraglia E, Pescarmona G, Ghigo D, Bosia A

Artemisinin induces doxorubicin resistance in human colon cancer cells via calcium-dependent activation of HIF-1? and P-glycoprotein overexpression

BRITISH JOURNAL OF PHARMACOLOGY (2009) 156(7)
DOI: 10.1111/j.1476-5381.2009.00117

Artemisinin induces doxorubicin resistance in human colon cancer cells via the calcium-dependent HIF-1α activation and P-glycoprotein overexpression

Running title: Artemisinin induces doxorubicin resistance

C. Riganti*[,1], S. Doublier*, D. Viarisio*, E. Miraglia*, G. Pescarmona*, D. Ghigo*, A. Bosia*

* Department of Genetics, Biology and Biochemistry, University of Torino, and Research Center on Experimental Medicine (CeRMS), Via Santena, 5/bis, 10126, Torino, Italy

[1] **Corresponding author:** Chiara Riganti, Dipartimento di Genetica, Biologia e Biochimica (Sezione di Biochimica), Via Santena, 5/bis, 10126 Turin, Italy. Phone: 39-11-670-5851; Fax: 39-11-670-5845; E-mail: chiara.riganti@unito.it

ABSTRACT

Background and purpose. Artemisinin is an antimalarial drug exerting pleiotropic effects, such as the inhibition of the transcription factor NF-kB and of the sarcoplasmic/endoplasmic reticulum Ca^{++}-ATPase (SERCA) of *P. falciparum*. Since the sesquiterpene lactone thapsigargin, a known inhibitor of mammalian SERCA, has been observed to enhance the expression of P-glycoprotein (Pgp) by increasing the intracellular Ca^{++} ($[Ca^{++}]_i$) level, we investigated whether artemisinin and its structural homolog parthenolide could inhibit SERCA in human colon carcinoma HT29 cells and induce a resistance to doxorubicin. **Experimental approach**. HT29 cells were incubated with artemisinin or parthenolide and evaluated as to SERCA activity, $[Ca^{++}]_i$ levels, Pgp expression, doxorubicin accumulation and toxicity, HIF-1α translocation. **Key results**. Artemisinin and parthenolide, similarly to the specific SERCA inhibitors thapsigargin and cyclopiazonic acid, reduced the activity of SERCA. They also increased the $[Ca^{++}]_i$ level and the Pgp expression and decreased the doxorubicin accumulation and cytotoxicity: the intracellular Ca^{++} chelator BAPTA and the inhibitor of calmodulin-dependent kinase II (CaMKII) KN93 prevented these effects. CaMKII is known to promote the phosphorylation and the activation of the hypoxia inducible transcription factor HIF-1α, which may induce Pgp: in HT29 cells artemisinin and parthenolide induced the phosphorylation of HIF-1α, which was inhibited by KN93. **Conclusions and Implications**. Our results suggest that artemisinin and parthenolide may behave as SERCA inhibitors, and like other SERCA inhibitors induce a doxorubicin resistance in human colon cancer cells, via the CaMKII-dependent activation of HIF-1α and the induction of Pgp.

Key words: artemisinin, sesquiterpene lactones, doxorubicin, colon cancer cells, calcium, HIF-1α, P-glycoprotein, calmodulin-dependent kinase II.

INTRODUCTION

The overexpression of the membrane pump P-glycoprotein (Pgp) in cancer cells is one of the main mechanisms of the multidrug resistance (MDR), an intrinsic or acquired cross-resistance toward

different chemotherapeutic drugs (Takara *et al*., 2006). Since MDR is the major obstacle to a successful cancer therapy, the mechanism of the transcription of the Pgp gene (*mdr1*) is the object of intense investigation (Takara *et al.*, 2006). The increase of cytosolic calcium ($[Ca^{++}]_i$) levels has been correlated to Pgp expression: in human lung Calu-3 cancer cells, the ouabain-dependent Pgp expression was blunted by the calcium chelator 1,2-bis(2-aminophenoxy)ethane-N,N,N',N'-tetraacetic acid (BAPTA), and the sesquiterpene lactone drug thapsigargin, a well known inhibitor of the mammalian sarcoplasmic/endoplasmic reticulum Ca^{++}-ATPase (SERCA) (Eckstein-Ludwig *et al*., 2003; Uhleman *et al*., 2005) enhanced the ouabain's effect (Baudouin-Legros *et al*., 2003). This means that, by increasing $[Ca^{++}]_i$, thapsigargin may regulate the transcription of the *mdr1* gene and enhance the expression of Pgp. An increase of $[Ca^{++}]_i$ is known also to activate the transcription factor hypoxia-inducible factor-1 (HIF-1) (Yuan *et al*., 2005; Hui *et al*., 2006), which controls several genes involved in cellular growth, glucose and iron metabolism, pH control, angiogenesis and matrix remodelling (O'Donnel *et al*., 2006), and is also involved in Pgp up-regulation (Comerford *et al*., 2002). HIF-1 is composed of two subunits: the β subunit is constitutively expressed, whereas the α subunit is rapidly degraded in normoxia, but becomes stable in hypoxia (O'Donnel *et al*., 2006) and its synthesis increases after stimulation with many growth factors and cytokines (Zhou and Brune, 2006).

Interestingly, another sesquiterpene lactone, artemisinin, which is widely used in the treatment of drug-resistant malaria (Hien *et al.*, 1993), inhibits the SERCA of *Plasmodium falciparum*, with a potency comparable to the one of thapsigargin (Eckstein-Ludwig *et al*., 2003; Uhleman *et al*., 2005). Artemisinin is known to exert pleiotropic effects, and the precise mechanism by which it kills *P. falciparum* has not been fully clarified (Golenser *et al*., 2006). For instance, in several cell types artemisinin inhibits the transcription factor nuclear factor-kappa B (NF-kB), a property exhibited also by other sesquiterpene compounds (Aldieri *et al*., 2003; Li *et al*., 2006).

In preliminary experiments we observed that artemisinin, as well as parthenolide, reduced the activity of SERCA and increased $[Ca^{++}]_i$ in human colon cancer HT29 cells, making them more

resistant to the toxic effects of doxorubicin. Starting from this observation, we decided to investigate whether these sesquiterpene lactones may up-regulate the Pgp expression in HT29 cells by inhibiting SERCA and by increasing $[Ca^{++}]_i$, thus inducing a doxorubicin-resistant phenotype, and whether these events could be related to HIF-1α activation.

MATERIALS AND METHODS

Materials. Foetal bovine serum (FBS), RPMI 1640, HAM's F12 and DMEM medium were supplied by BioWhittaker (Verviers, Belgium); plasticware for cell culture was from Falcon (Becton Dickinson, Bedford, MA). KN93 was purchased from Calbiochem (La Jolla, CA). Electrophoresis reagents were obtained from Biorad (Hercules, CA). When not otherwise specified, the other reagents were purchased from Sigma Chemical Co (St. Louis, MO).

Cells. Human colon doxorubicin-sensitive and cisplatin-sensitive cancer cells (HT29) (Riganti *et al.*, 2005) were cultured in RPMI 1640 supplemented with 10% FBS, 1% penicillin/streptomycin, 1% L-glutamine and maintained in a humidified atmosphere at 37°C, 5% CO_2 and 20 % O_2. To culture them in hypoxic conditions, HT29 cells were grown for 3 h in humidified atmosphere at 37°C, 5% CO_2 and 3 % O_2. Human colon cancer LoVo cells were cultured in HAM's F12 medium, human liver cancer HepG2 cells in RPMI 1640 medium and human breast cancer MCF-7 cells in a 1/1 (v/v) mixture of HAM's F12 and DMEM; each medium was supplemented with 10% FBS, 1% penicillin/streptomycin and 1% L-glutamine.

SERCA activity. Cells were lysed in buffer A (50 mM Hepes, 750 mM KCl, 200 mM sucrose, 10 mM $NaHCO_3$, pH 7.4), supplemented with protease inhibitor cocktail set III (Calbiochem) and centrifugated at 13,000 x g for 5 min. Supernatant was collected and centrifugated at 100,000 x g for 1 h at 4°C, then the pellet was resuspended in 1 ml of buffer B (20 mM Hepes, 160 mM KCl, 1 mM $MgCl_2$, 1 mM $CaCl_2$, 0.5% TritonX-100, pH 7.4); 100 μg of each sample were immunoprecipitated overnight with the rabbit polyclonal anti-SERCA 1/2/3 antibody (diluted 1: 100, Santa Cruz Biotechnology, Santa Cruz, CA). Samples were washed twice with 1 ml of buffer

B, supplemented with 2 mM DTT, then subjected to the following investigations. 10 µg of immunoprecipitated proteins were directly probed with the same antibody (diluted 1: 250, in PBS-BSA 1%, Santa Cruz Biotechnology), to measure total SERCA protein, while 50 µg were mixed with 2 mM ATP, 2.5 mM phosphoenolpyruvate, 7.5 U pyruvate kinase, 8.0 U lactate dehydrogenase, 0.2 mM calmodulin to check SERCA activity, as previously described (Krishna *et al.*, 2001). The reaction was started by adding 0.25 mM NADH and was followed for 10 min, measuring the absorbance at 340 nm with a Lambda 3 spectrophotometer (Perkin Elmer, Waltham, MA). The reaction kinetic was linear throughout the time of measurement. The NADH oxidation rate (expressed as µmol NADH oxidized/min/mg prot) of each sample was subtracted from that obtained in the absence of SERCA. The ATP hydrolysis rate was calculated stoichiometrically (Krishna *et al.*, 2001) and ATPase activity was expressed as µmol ATP hydrolyzed min^{-1} mg $prot^{-1}$.

$[Ca^{++}]_i$ measurement. Cells were grown 24 h on sterile glass coverslips, washed twice with PBS and incubated for 10 min at 37°C in Hepes-Ca buffer (10 mM Hepes, 145 mM NaCl, 1 mM $CaCl_2$, 5 mM KCl, 1 mM $MgSO_4$, 10 mM glucose, pH 7.4), with 10 µM calcium-sensitive fluorescent probe FURA acetoxymethylester (AM). After FURA-AM loading, coverslips were washed with Hepes-Ca buffer and firmly positioned in a quartz cuvette (1 cm) containing 1 ml of Hepes-Ca buffer. Either 10 µM parthenolide or 10 µM artemisinin was added when indicated. The cuvette holder was thermostatted at 37°C and the fluorescence of coverslips was measured in a Perkin-Elmer LS-5 spectrofluorimeter (Perkin Elmer). Excitation and emission wavelengths were 490 and 530 nm, respectively. Fluorescence was recorded for 1 h, during which the integrity of the monolayer was maintained, as assessed by measuring the extracellular LDH release (see the following paragraphs). Calculation of $[Ca^{++}]_i$ levels was performed as previously described (Hallam *et al.*, 1984). The fluorescence of Ca^{++}-saturated dye (F_{max}), obtained by treating cells with 10 µM ionomycin in Hepes-Ca buffer, was taken as the maximal emission. 2 mM $MnCl_2$ was then added to displace Ca^{++} from FURA and to obtain the value of FURA autofluorescence (F_{min}) alone. To prevent the $[Ca^{++}]_i$ increase, HT29 cells were pre-incubated for 1 h with 10 µM BAPTA

acetoxymethylester (BAPTA-AM) in order to load them with the Ca^{++} chelator BAPTA, then washed with PBS, and subjected to the same procedure of the other experimental points.

Cytochrome c release. Cells were washed twice in ice-cold PBS, then lysed in 0.5 ml buffer A (50 mM Tris, 100 mM KCl, 5 mM $MgCl_2$, 1.8 mM ATP, 1 mM EDTA; pH 7.2), supplemented with protease inhibitor cocktail set III (Calbiochem), 1 mM PMSF and 250 mM NaF. Mitochondrial and cytosolic fractions were separated as described (Wibom *et al.*, 2002). Samples were clarified by centrifuging at 650 x g for 3 min at 4°C, and the supernatant was collected and centrifuged at 13,000 x g for 5 min at 4°C. The new supernatant (cytosolic fraction) was transferred in other tubes, whereas the pellet (mitochondrial fraction) was rinsed with 0.5 ml buffer A, re-suspended in 0.25 ml buffer B (250 mM sucrose, 15 mM K_2HPO_4, 2 mM $MgCl_2$, 0.5 mM EDTA, 5% w/v BSA) and sonicated (two bursts of 10 seconds). 10 μg from each cytosolic or mitochondrial fraction were subjected to15% SDS-PAGE and probed with an anti-cytochrome c antibody (diluted 1:1,000 in PBS-BSA 1%, from Becton Dickinson).

Real time polymerase chain reaction (RT-PCR). Total RNA was obtained as previously described (Chomczynski and Sacchi, 1987). 5 μg of RNA were retro-transcribed by 200 U M-MLV reverse transcriptase (Invitrogen, Milan, Italy), in presence of 40 U/ μl RNAseOUT (Invitrogen). Real-time RT-PCR was carried out using IQ™ SYBR Green Supermix (Biorad), according to the manufacturer's instructions. The same cDNA preparation was used for the quantitation of Pgp and GAPDH, used as an housekeeping gene. The sequences of Pgp primers for quantitative RT-PCR were 5'-TGCTGGAGCGGTTCTACG-3', 5'-ATAGGCAATGTTCTCAGCAATG-3' (Invitrogen). Cycling for Pgp was: 1 cycle at 94°C for 2 min, followed by 45 cycles at 94°C for 30 s, annealing at 55°C for 30 s, extension at 72°C for 30 s. The sequences of GAPDH primers were 5'-GAAGGTGAAGGTCGGAGT-3', 5'-CATGGTGGAATCATATTGGAA-3' (Invitrogen). Cycling for GAPDH was: 1 cycle at 94°C for 2 min, followed by 40 cycles at 94°C for 30 s, annealing at 58°C for 30 s, extension at 72°C for 30 s. The relative quantitation of each sample was performed

comparing the Pgp PCR product with the GAPDH product, using the Biorad Software Gene Expression Quantitation (Biorad).

Western blot analysis. Pgp protein was detected by Western blotting as reported elsewhere (Riganti *et al.*, 2005). The densitometric analysis of the Western blots was performed with the Image J software (http://rsb.info.nih.gov/ij/). To assess HIF-1α phosphorylation, the whole cellular lysate was immunoprecipitated overnight with the mouse monoclonal anti-HIF-1α antibody (diluted 1: 250, Santa Cruz Biotechnology) and the immunoprecipitated proteins were separated by SDS-PAGE (10%), transferred to PVDF membrane sheets (Immobilon-P, Millipore, Bedford, MA) and probed with a biotin-conjugated anti-phosphoserine antibody (diluted 1:1,000 in TBS-BSA 3%, Sigma Chemical Co.) for 1 h. The membrane was washed in TBS-Tween 0.1% and subjected for 1 h to a streptavidin- and horseradish peroxidase-conjugated polimer (diluted 1:10,000 in TBS-BSA 3%, Sigma Chemical Co.). The membrane was washed again with TBS-Tween and proteins were detected by enhanced chemiluminescence (Immun-Star, Biorad).

Doxorubicin accumulation. Intracellular doxorubicin accumulation was measured by a fluorimetric assay as described elsewhere (Riganti *et al.*, 2005). Excitation and emission wavelengths were 475 and 553 nm. Fluorescence was converted in ng doxorubicin mg cell proteins^{-1}, using a calibration curve prepared previously.

Extracellular lactate dehydrogenase (LDH) activity. After a 6 h incubation under different experimental conditions in the presence of 5 μM doxorubicin, LDH activity was measured in the extracellular medium and in the cell lysate, as previously described (Riganti *et al.*, 2005), to check the cytotoxicity of doxorubicin. Absorbance at 340 nm was measured for 10 min with a Lambda 3 spectrophotometer (Perkin Elmer). Both intracellular and extracellular enzyme activity was expressed as μmol NADH oxidized min^{-1}, then extracellular LDH activity was calculated as percentage of the total LDH activity in the dish.

Trypan blue staining. After a 6 h incubation under different experimental conditions, cell monolayers were washed and let grow for other 24 h in fresh medium, then detached with

trypsin/EDTA and resuspended in 1 ml of PBS. 10 µl of 20% (w/v) trypan blue were added to each sample. After a 1 min incubation at room temperature, 10 µl of each cellular suspension were analyzed under a light microscope and the trypan blue-positive cells were counted as percentage of dead cells on a total number of 200 cells.

Annexin V/propidium iodide (PI) assay. Cells were incubated for 6 h in the experimental conditions described under the Results section, then they were washed and cultured for other 24 h in fresh medium. After this incubation time, cells were rinsed twice with fresh PBS, detached with the Cell Dissociation Solution (Sigma Chemical Co) and incubated for 10 min at room temperature in 1 ml of binding buffer (100 mM Hepes/NaOH, 140 mM NaCl, 25 mM $CaCl_2$, pH 7.5) containing 10 µM annexin V-fluorescein isothiocyanate conjugate (FITC) and 5 µM PI. The cell suspensions were washed three times with fresh PBS and rinsed with 1 ml of binding buffer. The fluorescence of each sample was recorded using a FACSCalibur system (Becton Dickinson). For each analysis 10,000 events were collected; the green fluorescence (for annexin V-FITC) was selected using a 530 nm band pass filter, while the red fluorescence (for PI) was obtained with a 640 nm longpass filter. The percentage of cells positive for annexin V, PI or both was calculated by the Cell Quest software (Becton Dickinson).

Cell cycle analysis. Cells, incubated for 6 h in the experimental conditions described under the Results section and cultured for the subsequent 24 h in fresh medium, were washed twice with fresh PBS, detached with the Cell Dissociation Solution (Sigma Chemical Co) and re-suspended in 100 µl of ice-cold PBS. Samples were incubated for 1h at 4°C in presence of 500 µl of 70% ethanol, then centrifuged at 1,200 x g for 5 min and rinsed with 300 µl of Citrate buffer (50 mM Na_2HPO_4, 25 mM sodium citrate, 0.1% Triton X-100), containing 10 µg/ml PI and 1 mg/ml RNAse (from bovine pancreas). After a 15 min incubation in the dark, the intracellular fluorescence was detected by a FACSCalibur system (Becton Dickinson). For each analysis 10,000 events were collected and a gate was drawn on the forward scatter/side scatter dot plot to exclude dead cells and debris. The results of the cell cycle analysis were elaborated by the Cell Quest software (Becton Dickinson).

Electrophoretic mobility shift assay (EMSA). Cells were plated in 60-mm diameter dishes at confluence and 10 μg of nuclear proteins were used to detect NF-kB translocation as described (Aldieri *et al*., 2003). The probe containing the HIF-1α oligonucleotide consensus sequence was labeled with [γ-^{32}P]ATP (Amersham Bioscience, Piscataway, NJ) (3,000 Ci/mmol, 250 μCi), using T4 polynucleotide kinase (Roche, Basel, Switzerland). The sequence of oligonucleotide was: 5'-TCTGTACGTGACCACACTCACCTC-3'; 3'-AGACATGCACTGGTGTGAGTGGAG-5' (Santa Cruz Biotechnology). 10 μg of extracts were incubated for 20 min with 20,000 cpm of ^{32}P-labeled double-stranded oligonucleotide at 4°C. The DNA-protein complex was separated on a not-denaturating 4% polyacrilamide gel in TBE buffer (0.4 M Tris, 0.45 M boric acid, 0.5 M EDTA, pH 8.0). After electrophoresis, the gel was dried and autoradiographed by exposure to X-ray film for 48 h.

Statistical analysis. All data in text and figures are provided as means ± SE. The results were analysed by a one-way Analysis of Variance (ANOVA) and Tukey's test. $p < 0.05$ was considered significant.

RESULTS

Artemisinin inhibits SERCA activity and increases $[Ca^{++}]_i$ levels in HT29 cells.

Artemisinin and the structurally related sesquiterpene lactone parthenolide, reduced SERCA activity in HT29 cells in a dose-dependent way (Figure 1). Artemisinin and parthenolide were less effective than thapsigargin and cyclopiazonic acid, two well-known SERCA inhibitors (Seidler *et al.*, 1989): however at 10 μM they significantly reduced the activity of SERCA (Figure 1). The expression of SERCA, detected by Western blotting in the immunoprecipitated samples, did not change under any experimental condition (data not shown). We then checked the $[Ca^{++}]_i$ levels in HT29 cells by using the fluorescent probe FURA-AM. Artemisinin and parthenolide elicited a significant transient of $[Ca^{++}]_i$ which reached the maximum value between 3 and 5 min after the drug addition (Figure 2A). Under each experimental condition the $[Ca^{++}]_i$ levels returned to the

baseline within 30 min (Figure 2A) and looked to be stable during a further 30 min period (not shown). When HT29 cells were pre-loaded with the Ca^{++} chelator BAPTA, none of these drugs was able to increase $[Ca^{++}]_i$ (Figure 2B). None of the drugs exerted a cytotoxic effect, since the release of LDH in the supernatant was not modified throughout the assay time in all the experimental conditions analysed (data not shown). To assess whether the increase of $[Ca^{++}]_i$ elicited by parthenolide and artemisinin was associated to the activation of an intrinsic pathway of apoptosis, we measured the realease of cytochrome c from mitochondria into the cytosol in HT29 cells incubated with artemisinin and parthenolide for different times (Figure 2C). In untreated cells, as well as after a 10 min incubation with the sesquiterpene lactones, cytochrome c was not released from mitochondria. Only after 30 min artemisinin and parthenolide induced a weak increase of cytosolic cytochrome c, which was still present after 1 h, but was no longer detectable after 3 h. When cells were pre-loaded with BAPTA, the release of cytochrome c was completely prevented (Figure 2C).

Artemisinin and parthenolide increase Pgp levels and reduce doxorubicin accumulation and toxicity in HT29 cells.

An increase of $[Ca^{++}]_i$ has been observed to potentiate the ouabain-induced expression of the mdr1/Pgp gene in a human lung cancer cell line (Baudouin-Legros *et al*., 2003). In HT29 cells, artemisinin and parthenolide significantly increased the Pgp mRNA as a function of time. Significantly higher mRNA levels were detectable after a 3 h incubation with each drug and increased further after a 6 h incubation (Figure 3A). A 3 h incubation with either artemisinin or parthenolide induced a slight increase of the amount of Pgp protein; a stronger induction was detected after a 6 h incubation (Figure 3B and Figure S1). The pre-incubation with BAPTA-AM prevented the increase of both Pgp mRNA and protein elicited by the drugs, without changing the basal expression of Pgp (Figure 3 and Figure S1). In parallel, a 6 h incubation with the drugs caused a significant decrease of intracellular doxorubicin accumulation and of doxorubicin toxicity (assessed as release of LDH) (Figure 4A): a 1 h pre-incubation with BAPTA-AM completely

prevented both the effects elicited by the drugs. In the absence of doxorubicin none of these agents exerted a significant increase of LDH activity in the culture medium (data not shown). In the presence of the drugs, the number of trypan blue-positive or annexin V- and PI-positive cells was strongly reduced in comparison with the HT29 cells treated with doxorubicin alone (Figure 4B and Figure S2); however, the pre-incubation with BAPTA-AM prevented the effects of SERCA inhibitors on cell viability and apoptosis (Figure 4B and Figure S2). We then investigated whether artemisinin or parthenolide might affect the cell-cycle arrest induced by doxorubicin. HT29 cells were incubated for 6 h in the presence of doxorubicin, with or without one of the sesquiterpene drugs, then washed and let grow for further 24 h in fresh medium. After this incubation time, cells were permeabilized and assessed for the cell cycle phases by FACS analysis. Doxorubicin lowered the percentage of cells entering the S phase toward the untreated cells, as shown in Figure 4C and in Figure S2. When doxorubicin was co-incubated with either artemisinin or parthenolide, the percentage of cells in S phase remained significantly higher than that found in cells treated with doxorubicin alone (Figure 4C). Again, the cell loading with BAPTA completely abrogated the effect of the drugs on cell cycle. The number of cells in G_0/G_1 and G_2/M phase did not change under any experimental conditions (Figure 4C and Figure S2).

The inhibition of calmodulin kinase II (CaMKII) reverts the effect of artemisinin and parthenolide on Pgp expression and doxorubicin accumulation and toxicity.

In order to investigate the mechanism which may associate the increase of $[Ca^{++}]_i$ to the Pgp induction, we incubated HT29 cells with KN93, which is known to inhibit the calmodulin-dependent kinase II (CaMKII) (Kuhn *et al*., 1980; Zhu *et al*., 2003). KN93 prevented the increase of Pgp gene transcription (Figure 5A) and of Pgp protein expression (Figure 5B and Figure S1) elicited by artemisinin and parthenolide at each time point. In parallel, the reduction of doxorubicin's accumulation, cytotoxicity and pro-apoptotic effect exerted by the different drugs was completely blunted in the presence of KN93 (Figure 6 and Figure S2). Similarly, the CaMKII inhibitor abrogated the effects of the sesquiterpene drugs on the cell cycle progression, measured in

the cells incubated for 6 h with doxorubicin or parthenolide/artemisinin, and then cultured for further 24 h in fresh medium (Figure 6 C and Figure S2). When used alone, KN93 did not significantly affect Pgp mRNA and protein expression (Figure 5 and Figure S1), intracellular doxorubicin accumulation and doxorubicin-induced extracellular release of LDH. Moreover it changed neither the number of HT29 cells positive for trypan blue and annexin V/PI nor the percentage of cells entering the S phase (Figure 6, Figure S2).

The transcription factor HIF-1α is activated by artemisinin and parthenolide via CaMKII in HT29 cells.

It has been reported that CaMKII promotes the phosphorylation and the nuclear translocation of HIF-1α (Yuan *et al*., 2005). In HT29 cells the incubation with either artemisinin or parthenolide induced the phosphorylation of HIF-1α, which was absent in untreated cells and inhibited in the presence of KN93 (Figure 7A). By EMSA assay, in the same experimental conditions we observed a very slight binding of HIF-1α to DNA in non-stimulated cells (Figure 7B), whereas, after incubation with either artemisinin or parthenolide, the nuclear translocation of HIF-1α was significantly enhanced (Figure 7B). A similar increase was obtained after a 3 h incubation in hypoxic conditions, taken as a positive control. In the presence of KN93, no increase of HIF-1α translocation was elicited by artemisinin and parthenolide. Our results suggest that these drugs promote in HT29 cells the phosphorylation and the nuclear translocation of HIF-1α via CaMKII (Figure 7A and B).

DISCUSSION AND CONCLUSIONS

Since the first isolation from *Artemisia annua* in 1972, artemisinin, also known as qinghaosu, has reached a worldwide diffusion as antimalarial drug (Golenser *et al*., 2006). Different hypotheses have been made as to its mechanism of action: the drug has been proposed to alter the redox balance of *P. falciparum*, to interfere with parasite transport proteins, to disrupt the parasite mitochondrial function and to modulate the host immune function (Golenser *et al*., 2006). Artemisinin has been

shown to bind and to inhibit the PfATP6 protein (the SERCA orthologue of *P. falciparum*), similarly to thapsigargin, a sesquiterpene lactone already known to inhibit protozoan and mammalian SERCA (Eckstein-Ludwig *et al*., 2003; Uhleman *et al*., 2005).

In our work we first investigated whether artemisinin inhibits SERCA activity and increases $[Ca^{++}]_i$ also in a mammalian cell line, the human colon cancer HT29 cells, in comparison with thapsigargin and cyclopiazonic acid, two well known SERCA inhibitors (Seidler *et al*., 1989). We analyzed also the effect of parthenolide, a sesquiterpene lactone structurally similar to artemisinin, which exhibits pro-apoptotic (Kim *et al*., 2005), anti-inflammatory and anti-septic (Aldieri *et al*., 2003; Li *et al*., 2006) properties. In our experiments both artemisinin and parthenolide reduced the activity of purified SERCA, although less potently than the known SERCA inhibitors thapsigargin and cyclopiazonic acid. The small differences in the chemical structure of these drugs may account for this discrepancy. At the concentration of artemisinin used in the present work (10 μM), the inhibition of SERCA is expected to be specific: indeed when PfATP6 is expressed in *Xenopus laevis* oocytes, no other transporters are inhibited even at 50 μM artemisinin (Eckstein-Ludwig *et al*., 2003).

As a consequence of SERCA inhibition, artemisinin is supposed to elicit an increase of $[Ca^{++}]_i$ in HT29 cells. A previous work has reported that artemisinin increases the transient of $[Ca^{++}]_i$ induced by 60 mM KCl in guinea pig ventricular myocytes (Ai *et al*., 2001). In our experimental conditions artemisinin, as well as parthenolide, induced a significant increase of basal $[Ca^{++}]_i$ with a superimposable kinetics. To our knowledge, this is the first work reporting that artemisinin may inhibit SERCA pumps and increase $[Ca^{++}]_i$ levels in human cells. This increase was followed by a weak release of cytochrome c from mithocondria into cytosol, an index of the activation of an intrinsic apoptotic pathway in cells. The peak of $[Ca^{++}]_i$ increase preceded the peak of the cytochrome c release, as expected, and both events showed to decline rapidly after having reached the maximum. We may hypothesize that, since the $[Ca^{++}]_i$ level declined toward the baseline 5 min after the exposure to the drug, cells were exposed to a pro-apoptotic signal for a very short time.

The cytochrome c is usually degraded by proteasome (Ferraro *et al*, 2008), allowing the activation of the anti-apoptotic programs and the cell survival. Indeed we did not detect any significant increase of LDH activity in the extracellular medium in the presence of either parthenolide or artemisinin alone: this result may suggest that the increase of $[Ca^{++}]_i$ levels elicited by the sesquiterpene drugs triggers a weak activation of the intrinsic pro-apoptotic pathway, which does not lead to a significant cell death of HT29 cells.

The increase of $[Ca^{++}]_i$ levels has been correlated to mdr1/Pgp gene expression: in human lung cancer cells, thapsigargin enhances the ouabain-dependent Pgp expression and this effect is blunted by the calcium chelator BAPTA (Baudouin-Legros *et al*., 2003). Untreated HT29 cells express very low amounts of Pgp mRNA and protein: artemisinin and parthenolide increased the level of cytosolic $[Ca^{++}]_i$ and enhanced the Pgp gene transcription and protein expression. The effects on both mRNA and protein were time-dependent for both drugs. These sesquiterpene lactones also reduced the intracellular accumulation of doxorubicin and the cytotoxic effects of doxorubicin in HT29 cells, as far as LDH release, decrease of cell viability, induction of apoptosis and cell cycle derangement were concerned.

Recently, a great interest has grown about the possibility of using natural terpenes in the treatment of MDR. For instance, it has been shown that some natural terpenes reduce rhodamine efflux in mouse lymphoma cells and in multidrug resistant human breast cancer cells (Molnár *et al*., 2006). Different sesquiterpenes modulate the activity of *Leishmania tropica* Pgp, which shows 37% homology with mammalian Pgp (Cortés-Selva *et al*., 2005). However, no data are available as to a direct effect of sesquiterpenes on Pgp mRNA levels and protein expression.

We hypothesize that Ca^{++} mobilization may be responsible for the increase of Pgp gene transcription. Indeed, in the presence of BAPTA, artemisinin and parthenolide did not induce a significant $[Ca^{++}]_i$ change in HT29 cells and did not increase the Pgp expression. The $[Ca^{++}]_i$ levels seem to play a key role in regulating doxorubicin efficacy in HT29 colon cancer cells, as no

inhibition of the intracellular doxorubicin accumulation and of the doxorubicin cytotoxicity was observed in the presence of BAPTA.

A rapid increase of $[Ca^{++}]_i$ have pleiotropic effects on human cells (Chen *et al*., 2003). For instance, calcium may enhance the transcription of several genes through the activation of the CaMK proteins, the Ras/Raf/MEK/extracellular signal regulated (ERK/RSK) kinases and the cyclic AMP response element (CRE)-binding protein (CREB) (Chen *et al*., 2003). In HT29 cells the sesquiterpene lactone-induced $[Ca^{++}]_i$ increase was transient and returned to the baseline after a few minutes. This rapid increase of $[Ca^{++}]_i$ may activate calmodulin and CaMKII, as inferred by the inhibitory effect of KN93. CaMKII is a pleiotropic mediator of calcium signalling and its activity is a fine sensor of the $[Ca^{++}]_i$ increase (Dupont *et al*., 2003). In HT29 cells the addition of the CaMKII inhibitor KN93 abolished the up-regulation of Pgp elicited by artemisinin and parthenolide, and made the drug-stimulated cells as sensitive to doxorubicin's effects as resting cells. Taken together, our results suggest that CaMKII could affect the activity of a transcription factor acting on the mdr1 gene promoter.

Different transcription factor binding sites are located on mdr1 gene (Takara *et al*., 2006). Among them, an hypoxia responsive element (HRE) specific for HIF-1α has been identified (Comerford *et al*., 2002). Hypoxic areas of tumors are more resistant to chemotherapeutic drugs, due to their enhanced expression of Pgp (O'Donnel *et al*., 2006). Moreover, the increased synthesis of cytokines and hormones and the activation of different tyrosine kinase receptors may elevate HIF-1α activity even in normoxic cancer cells (Zhou and Brune, 2006). Changes of the intracellular calcium levels have been variously related to HIF-1α activation (Berchner-Pfannschmidt *et al*., 2004; Yuan *et al*., 2005). For instance, the HIF-1α expression and activity is enhanced by the calcium-induced activation of PKC-α (Hui *et al*., 2006). HIF-1α may be phosphorylated on serine by different kinases (O'Donnel *et al*., 2006), which enhance HIF-1α activity or stability, up-regulating the target genes controlled by HRE (Sodhi *et al*., 2001; Suzuki *et al*., 2001). Interestingly, in rat pheochromocytoma cells the CaMKII activation significantly induces the transcription of HIF-1α -

dependent genes under normoxic conditions (Yuan *et al*., 2005). Our results show that also in human HT29 colon cancer cells, expressing very low basal levels of HIF-1α, the drugs eliciting a transient increase of $[Ca^{++}]_i$ induced a clear nuclear translocation, phosphorylation and DNA-binding activity of HIF-1α. Since the CaMKII inhibitor KN93 completely prevented such effects, we hypothesize that CaMKII may control both the activation of HIF-1α and the transcription of the mdr1 gene in HT29 cells.

In summary our results show that artemisinin and parthenolide are able to inhibit SERCA activity and to increase the $[Ca^{++}]_i$ levels in HT29 cells. The transient increase of $[Ca^{++}]_i$ may activate CaMKII, which in turn phosphorylates and activates the transcription factor HIF-1α. As a consequence of HIF-1α nuclear translocation, the Pgp is overexpressed, the doxorubicin intracellular accumulation is reduced and the doxorubicin cytotoxic effects are prevented. Therefore HT29 cells, when treated with artemisinin and parthenolide, become more resistant to doxorubicin. Our results were not cell type-specific: artemisinin and parthenolide decreased with similar mechanisms the efficacy of doxorubicin in human colon cancer LoVo cells, in human liver cancer HepG2 cells and in human breast cancer MCF-7 cells (Figures S3-S8). Furthermore, the same effects elicited by artemisinin and parthenolide were also exerted by the SERCA inhibitors thapsigargin and cyclopiazonic acid (data not shown). Therefore, the SERCA activity and the regulation of $[Ca^{++}]_i$ are likely to play a crucial role in Pgp expression and doxorubicin resistance in human cancer cells. In addition to their anti-malarial properties, artemisinin and its derivatives are cytotoxic for cancer cells and the pleiotropic nature of their antitumor effect has been recently discussed (Efferth, 2006; Nakase *et al*, 2007). It has been observed that the artemisinin derivative artesunate is similarly active towards drug-sensitive and multidrug resistant cell lines which overexpress Pgp (Efferth, 2006). Due to its antiproliferative and antiangiogenic properties, parthenolide has been proposed as an adjuvant drug in chemotherapy (Sweeney *et al*, 2005); a phase I clinical trial has shown the safety of orally administered parthenolide in cancer patients (Curry *et al*, 2004).

Our results suggest that artemisinin and parthenolide could interfere with the action of antineoplastic drugs, when administered together, making cancer cells more resistant to chemotherapy. At present parthenolide is only employed in preclinical and clinical trials, whereas the number of patients assuming artemisinin for malaria therapy or prophylaxis is high (Mohanty *et al*, 2006). Due to their broad therapeutic activity, anthracyclines are widely used in clinical protocols and often represent the first-line therapy against solid and haematological malignancies (Cortes-Funes and Coronado, 2007). Clinicians should take into account that the efficacy of doxorubicin might be reduced in patients subjected to a concomitant artemisinin therapy.

ACKNOWLEDGEMENT

This work has been supported with grants from Fondazione Internazionale Ricerche Medicina Sperimentale (FIRMS), Compagnia di San Paolo, Regione Piemonte (Ricerca Sanitaria Finalizzata CIPE A201 2004/2005 e 2006) and Ministero dell'Università e della Ricerca.

Sophie Doublier is recipient of a Research Fellowship funded by the Fondazione Internazionale Ricerche Medicina Sperimentale (FIRMS), Torino, Italy.

REFERENCES

- Ai J, Gao HH, He SZ, Wang L, Luo DL, Yang BF (2001). Effect of matrine, artemisinin and tetrandrine on cytosolic $[Ca^{2+}]_i$ in guinea pig ventricular myocytes. *Acta Pharmacol Sin* **22**: 512-516.
- Aldieri E, Atragene D, Bergandi L, Riganti C, Costamagna C, Bosia A, et al (2003). Artemisinin inhibits inducile nitric oxid sinthase and nuclear factor NF-kB activation. *FEBS Lett* **552**: 141-144.
- Baudouin-Legros M, Brouillard F, Tondelier D, Hinzpeter A, Edelman A (2003). Effect of ouabain on CFTR gene expression in human Calu-3 cells. *Am J Physiol Cell Physiol* **284**: C620-C626.

- Berchner-Pfannschmidt U, Petrat F, Doege K, Trinidad B, Freitag P, Metzen E, et al (2004). Chelation of Cellular Calcium Modulates Hypoxia-inducible Gene Expression through Activation of Hypoxia-inducible Factor-1 α. *J Biol Chem* **279**: 44976-44986.
- Beutler E (1971). Red cell metabolism. A manual of biochemical methods. New York: Grune & Stratton, pp 56-68.
- Chen Y, Zhuang S, Cassenaer S, Casteel DE, Gudi T, Boss GR, et al (2003). Synergism between Calcium and Cyclic GMP in Cyclic AMP Response Element-Dependent Transcriptional Regulation Requires Cooperation between CREB and C/EBP-β. *Mol Cell Biol* **23**: 4066-4082.
- Chomczynski P, Sacchi N (1987). Single-step method of RNA isolation by acid guanidinium thiocyanate-phenol-chloroform extraction. *Anal Biochem* **162**: 156-159.
- Comerford KM, Wallace TJ, Karhausen J, Louis NA, Montalto MC, Colgan SP (2002). Hypoxia-inducible Factor-1-dependent Regulation of the Multidrug Resistance (MDR1) Gene. *Cancer Res* **62**: 3387-3394.
- Cortes-Funes H, Coronado C (2007). Role of anthracyclines in the era of targeted therapy. *Cardiovasc Toxicol* **7:** 56-60.
- Cortés-Selva F, Jiménez IA, Muñoz-Martínez F, Campillo M, Bazzocchi IL, Pardo L, et al (2005). Dihidro-b-Agarofuran Sesquiterpenes: A New Class of Reversal Agents of the Multidrug Resistance Phenotype Mediated by P-Glycoprotein in the Protozoan Parasite Leishmania. *Cur Pharm Des* **11**: 3125-3139.
- Curry EA, Murry DJ, Yoder C, Fife K, Armstrong V, Nakshatri H, et al (2004). Phase I dose escalation trial of feverfew with standardized doses of parthenolide in patients with cancer. *Invest New Drugs* **22:** 299-305.
- Dupont G, Houart G, De Koninc P (2003). Sensitivity of CaM kinase II to the frequency of Ca2+ oscillations: a simple model. *Cell Calcium* **34**: 485-497.

- Eckstein-Ludwig U, Webb RJ, van Goethem IDA, East JM, Lee AG, Kimura M, et al (2003). Artemisinins target the SERCA of Plasmodium falciparum. *Nature* **424**: 957-961.
- Efferth T (2006). Molecular pharmacology and pharmacogenomics of artemisinin and its derivatives in cancer cells. *Curr Drug Targets* **7**: 407-421.
- Ferraro E, Pulicati A, Cencioni MT, Cozzolino M, Navoni F, di Martino S, et al (2008). Apoptosome-deficient Cells Lose Cytochrome *c* through Proteasomal Degradation but Survive by Autophagy-dependent Glycolysis. *Mol Biol Cell* **19**: 3576-3588.
- Golenser J, Waknine JH, Krugliak M, Hunt NH, Grau GE (2006). Current perspectives on the mechanism of action of artemisinins. *Int J Parasitol* **36**: 1427-1441.
- Hallam TJ, Sanchez A, Rink TJ (1984). Stimulus-response coupling in human platelets. Changes evoked by platelet-activating factor in cytoplasmic free calcium monitored with the fluorescent calcium indicator quin2. *Biochem J* **218**: 819-827.
- Hien T T, White N J (1993). Qinghaosu. *Lancet* **341**: 603-608.
- Hui AS, Bauer AL, Striet JB, Schnell PO, Czyzyk-Krzeska MF (2006). Calcium signaling stimulates translation of HIF-1a during hypoxia. *FASEB J* **20**: 466-475.
- Kim JH, Liu L, Lee S-O, Kim Y-T, You K-R, Kim D-G (2005). Susceptibility of Cholangiocarcinoma Cells to Parthenolide-Induced Apoptosis. *Cancer Res* **65**: 6312-6320.
- Krishna S, Woodrow C, Webb R, Penny J, Takeyasu K, Kimura M, et al (2001). Expression and Functional Characterization of a *Plasmodium falciparum* Ca21-ATPase (PfATP4) Belonging to a Subclass Unique to Apicomplexan Organisms. *J Biol Chem* **276**: 10782-10787.
- Kuhn DM, O'Callaghan JP, Juskevich J, Lovenberg W (1980). Activation of brain tryptophan hydroxylase by ATP-Mg^{2+}: Dependence on calmodulin. *Proc Natl Acad Sci USA* **77**: 4688-4691.

- Li W, Dong Y, Tu Y, Lin Z (2006). Dihydroarteannuin ameliorates lupus symptom of BXSB mice by inhibiting production of TNF-alpha and blocking the signalling pathway NF-kappa B translocation. *Int Immunopharmacol* **6**: 1243-1250.
- Mohanty S, Patel DK, Pati SS, Mishra SK (2006). Adjuvant therapy in cerebral malaria. *Indian J Med Res*,**124**: 245-60.
- Molnár J, Gyémánt N, Tanaka M, Hohmann J, Bergmann-Leitner E, Molnár P, et al (2006). Inhibition of Multidrug Resistance of Cancer Cells by Natural Diterpenes, Triterpenes and Carotenoids. *Curr Pharm Des* **12**: 287-311.
- Nakase I, Lai H, Singh NP, Sasaki T (2008). Anticancer properties of artemisinin derivatives and their targeted delivery by transferring conjugation. *Int J Pharmaceut*, **354:** 28-33.
- O'Donnell JL, Joyce MR, Shannon AM, Harmey J, Geraghty J, Bouchier-Hayes D (2006). Oncological implications of hypoxia inducible factor-1a (HIF-1a) expression. *Cancer Treat Rev* **32**: 407-416.
- Riganti C, Miraglia E, Viarisio D, Costamagna C, Pescarmona GP, Ghigo D, et al (2005). Nitric oxide reverts the resistance to doxorubicin in human colon cancer cells by inhibiting the drug efflux. *Cancer Res* **65**: 516-525.
- Seidler NW, Jonaz I, Veghg M, Martonosill A (1989). Cyclopiazonic Acid Is a Specific Inhibitor of the Ca2+-ATPase of Sarcoplasmic Reticulum. *J Biol Chem* **264**: 17816-17823.
- Sodhi A, Montaner S, Miyazaki H, Gutkind JS (2001). MAPK and Akt Act Cooperatively but Independently on Hypoxia Inducible Factor-1a in rasV12 Upregulation of VEGF. *Biochem Biophys Res Commun* **287**: 292-300.
- Suzuki H, Tomida A, Tsuruo T (2001). Dephosphorylated hypoxia inducible factor 1a as a mediator of p53-dependent apoptosis during hypoxia. *Oncogene* **20**: 5779-5788.

- Sweeney CJ, Mehrotra S, Sadaria MR, Kumar S, Shortle NH, Roman Y, et al (2005). The sesquiterpene lactone parthenolide in combination with docetaxel reduces metastasis and improves survival in a xenograft model of breast cancer. *Mol Cancer Ther*, **4**: 1004-12.
- Takara K, Sakaeda T, Okumura K (2006). An Update on Overcoming MDR1-Mediated Multidrug Resistance in Cancer Chemotherapy. *Curr Pharm Des* **12**: 273-286.
- Uhleman AC, Cameron A, Eckstein-Ludwig U, Fischbarg J, Iserovich P, Zuniga FA, et al (2005). A single aminoacid residue can determine the sensitivity of SERCA to artemisinins. *Nature Struct Mol Biol* **12**: 628-629.
- Wibom R, Hagenfeldt L, von Dobeln U. Measurement of ATP production and respiratory chain enzyme activities in mitochondria isolated from small muscle biopsy samples (2002). *Anal Biochem* **311**: 139-151.
- Yuan G, Nanduri J, Raman Bhasker C, Semenza GL, Prabhakar NR (2005). $Ca2^{++}$/Calmodulin Kinase-dependent Activation of Hypoxia Inducible Factor 1 Transcriptional Activity in Cells Subjected to Intermittent Hypoxia. *J Biol Chem* **280**: 4321-4328.
- Zhou J, Brüne B (2006). Cytokines and Hormones in the Regulation of Hypoxia Inducible Factor-1α (HIF-1 α). *Cardiovasc Hematol Agents Med Chem* **4**: 189-197.
- Zhu WZ, Wang SQ, Chakir K, Yang D, Zhang T, Brown JH, et al (2003). Linkage of α1-adrenergic stimulation to apoptotic heart cell death through protein kinase A–independent activation of Ca2+/calmodulin kinase II. *J Clin Invest* **111**: 617-625.

Supplementary information is available at the British Journal of Pharmacology website.

FIGURE LEGENDS

Figure 1. Effects of thapsigargin, parthenolide, artemisinin and cyclopiazonic acid on SERCA activity in HT29 cells. 50 µg of purified SERCA protein (see Materials and Methods) were incubated in the absence or presence of of thapsigargin (*thaps*, *open square*), parthenolide (*part*, *open circle*), artemisinin (*art*, *solid circle*), cyclopiazonic acid (*cpa*, *triangle*), at different concentrations. SERCA activity was measured as described under the Materials and Methods section. Measurements were performed in duplicate and data are presented as means $\pm$ SE (n = 4). SERCA activity in control cells was 4.82 $\pm$ 0.13 µmol ATP hydrolyzed/min /mg prot (n = 4; not shown in the figure). Significance vs *CTRL*: * $p < 0.001$.

Figure 2. Effects of parthenolide and artemisinin on $[Ca^{++}]_i$.

A. Cells were grown on sterile glass coverslips for 24 h, washed with PBS and incubated for 10 min in Hepes-Ca buffer containing 10 µM FURA-AM, in the absence (*ctrl*) or presence of either parthenolide (*part*, 10 µM) or artemisinin (*art*, 10 µM). Fluorescence was detected throughout the first 30 min, as described under Materials and Methods. Measurements were performed in duplicate and data are presented as means $\pm$ SE (n = 6). Significance of each drug vs *CTRL*: * $p < 0.005$.

B. Cells were grown on sterile glass coverslips as described previously, incubated for 1 h with 10 µM BAPTA-AM, then washed with PBS, and subjected to the same experimental procedure described in panel **A**. Measurements were performed in duplicate and data are presented as means $\pm$ SE (n = 4).

C. Cells were incubated for different times in the absence (*CTRL*) or in the presence of either parthenolide (*PART*, 10 µM) or artemisinin (*ART*, 10 µM). When indicated, cells were pre-loaded with the Ca^{++} chelator BAPTA (*BAP*) (see above). As a positive control, several samples were previously incubated for 24 h with the pro-apoptotic drug camptothecin (*CP*, 10 nM). Cytosolic and mitochondrial fractions were separated and subjected to Western blotting analysis for cytochrome c,

as described under Materials and Methods. The figure is representative of three experiments with similar results.

Figure 3. Effects of parthenolide and artemisinin on Pgp expression. HT29 cells were incubated for 1, 3 and 6 h in the absence (*CTRL*) or presence of either parthenolide (*PART*, 10 μM) or artemisinin (*ART*, 10 μM). When indicated, cells were pre-incubated for 1 h with BAPTA-AM (*BAP*, 10 μM), then washed in PBS and incubated in the absence or presence of one of the drugs as described above.

A. Total RNA was extracted and retro-transcribed by RT-PCR, performed at 1 h (*open bars*), 3 h (*hatched bars*) and 6 h (*solid bars*) as indicated under the Materials and Methods section. Measurements were performed in triplicate and data are presented as means $\pm$ SE (n = 3). Vs *CTRL*: * $p < 0.05$. Vs *PART* or *ART* respectively: $^{\circ}$ $p < 0.05$.

B. To detect the Pgp protein, cells were lysed and the whole cellular lysate was immunoprecipitated with an anti-Pgp polyclonal antibody. The immunoprecipitated proteins were subjected to Western blotting, using the same antibody (see Materials and Methods). The expression of GAPDH, the product of an housekeeping gene, was used as a control of equal protein loading. The figure is representative of three experiments with similar results.

Figure 4. Effects of parthenolide and artemisinin on doxorubicin accumulation and cytotoxicity (detected as: LDH release, trypan blue staining, percentage of apoptotic cells, percentage of cells in cycle). HT29 cells were cultured in the absence (*CTRL*) or in the presence of doxorubicin (5 μM, *DOX*) for 6 h, together with parthenolide (*PART*, 10 μM) or artemisinin (*ART*, 10 μM); when indicated, cells were pre-incubated for 1 h with BAPTA-AM (*BAP*, 10 μM), then washed in PBS before the incubation with the other drugs. **A.** Doxorubicin intracellular accumulation (*open bars*) and release of LDH activity in the culture supernatant (*hatched bars*) were measured as described

under Materials and Methods. Measurements were performed in duplicate and data are presented as means ± SE (n = 4). The significance of *DOX* vs *CTRL* was $p < 0.001$ (not reported in the figure). Vs *DOX*: * $p < 0.001$. Vs DOX+*PART* or DOX+*ART* respectively: ° $p < 0.02$. **B.** Trypan blue staining (*open bars*) and FACS analysis of annexin V-FITC and PI-positive HT29 cells (*hatched bars*) were performed as reported in the Materials and Methods section. Measurements were performed in duplicate and data are presented as means ± SE (n = 3). The significance of *DOX* vs *CTRL* was $p < 0.001$ (not reported in the figure). Vs *DOX*: * $p < 0.001$. Vs DOX+*PART* or DOX+*ART* respectively: ° $p < 0.001$. **C.** Cells were incubated for 6 h as indicated above, then washed and let grow for further 24 h in fresh medium; after this time, cells were permeabilized and treated with PI, as described under Materials and Methods. Cell cycle analysis of G_0/G_1 phase (*open bars*), S phase (*hatched bars*) and G_2/M phase (*solid bars*) was obtained by the FACSCalibur system using the Cell Quest software (see Materials and Methods for details). The measurements were performed in duplicate and data are presented as means ± SE (n = 3). Concerning the percentage of cells in S phase, the significance of *DOX* vs *CTRL* was $p < 0.05$ (not reported in the figure). Vs *DOX*: * $p < 0.05$. Vs DOX+*PART* or DOX+*ART* respectively: ° $p < 0.05$.

Figure 5. Effect of the CaMK II inhibitor KN93 on Pgp mRNA and protein expression. HT29 cells were incubated for 1 h, 3 h or 6 h in the absence (*CTRL*) or presence of either parthenolide (*PART*, 10 μM) or artemisinin (*ART*, 10 μM), alone or together with KN93 (*KN*, 10 μM). At the end of the incubation time, cells were subjected to the following investigations.

A. Total RNA was extracted and RT-PCR was performed at 1 h (*open bars*), 3 h (*hatched bars*) and 6 h (*solid bars*) as indicated under the Materials and Methods section. Measurements were performed in triplicate and data are presented as means ± SE (n = 3).Vs *CTRL*: * $p < 0.05$. Vs *PART* or *ART* respectively: ° $p < 0.05$.

B. Pgp was immunoprecipitated from the whole cellular lysate using an anti-Pgp antibody, then subjected to Western blotting as described under Materials and Methods. The expression of GAPDH was used as a control of equal protein loading. The figure is representative of three experiments with similar results.

Figure 6. Effect of the CaMK II inhibitor KN93 on doxorubicin accumulation and cytotoxicity (detected as: LDH release, trypan blue staining, percentage of apoptotic cells, percentage of cells in cycle). HT29 cells were in the absence (*CTRL*) or in the presence of doxorubicin (5 μM, *DOX*) for 6 h, together with either parthenolide (*PART*, 10 μM) or artemisinin (*ART*, 10 μM), alone or together with KN93 (*KN*, 10 μM). **A.** The cells were tested for the intracellular doxorubicin accumulation (*open bars)*, while the extracellular culture medium was checked for LDH activity (*hatched bars*) as previously indicated (see Materials and Methods). Measurements were performed in duplicate and data are presented as means $\pm$ SE (n = 3). The significance of *DOX* vs *CTRL* was $p < 0.001$ (not reported in the figure). Vs *DOX*: * $p < 0.05$. Vs DOX+*PART* or DOX+*ART* respectively: $^{\circ}$ $p < 0.05$.

B. Cells were stained with trypan blue (*open bars*) and assessed for the positivity of annexin V and PI by FACS analysis (*hatched bars*), as reported in the Materials and Methods section. The measurements were performed in duplicate and data are presented as means $\pm$ SE (n = 3). The significance of *DOX* vs *CTRL* was $p < 0.001$ (not reported in the figure).Vs *DOX*: * $p < 0.001$. Vs DOX+*PART* or DOX+*ART* respectively: $^{\circ}$ $p < 0.001$. **C.** Cells were incubated for 6 h as indicated above, then washed and let grow for further 24 h in fresh medium; after this time, cells were permeabilized and stained with PI, as described under Materials and Methods. The percentage of HT29 cells in G_0/G_1 phase (*open bars*), S phase (*hatched bars*) and G_2/M phase (*solid bars*) was measured by the FACSCalibur system using the Cell Quest software (see Materials and Methods for details). The measurements were performed in duplicate and data are presented as means $\pm$ SE (n = 3). As far as the percentage of cells in S phase is concerned, the significance of *DOX* vs *CTRL*

was $p < 0.05$ (not reported in the figure). Vs *DOX*: * $p < 0.05$. Vs DOX+*PART* or DOX+*ART* respectively: ° $p < 0.05$.

Figure 7. Effect of parthenolide, artemisinin and KN93 on HIF-1α phosphorylation and nuclear translocation. HT29 cells were incubated for 3 h in the absence (*CTRL*) or in the presence of either parthenolide (*PART*, 10 μM) or artemisinin (*ART*, 10 μM), alone or together with KN93 (*KN*, 10 μM), then the following investigations were performed.

A. Western blotting detection of phospho(Ser)-HIF-1α (pHIF-1α). Whole cell lysates were incubated with an anti-HIF-1α antibody, subsequently the immunoprecipitated proteins were separated by SDS-PAGE and probed with an anti-phosphoserine antibody as described under the Materials and Methods section. The expression of GAPDH was used as a control of equal protein loading. The figure is representative of three experiments with similar results.

B. EMSA detection of HIF-1α nuclear translocation. EMSA was performed on nuclear extracts as detailed under Materials and Methods. In each experiment one lane was loaded with bidistilled water (-) in place of cellular extracts. The lane marked with *HYP* was loaded with nuclear extracts obtained from HT29 cells incubated for 3 h in a humidified hypoxic atmosphere (3% O_2, 5% CO_2, 37 °C), to achieve a maximal HIF-1α activation. The figure is representative of three experiments with similar results.

Statement of conflict of interest.

None.

Figure 1

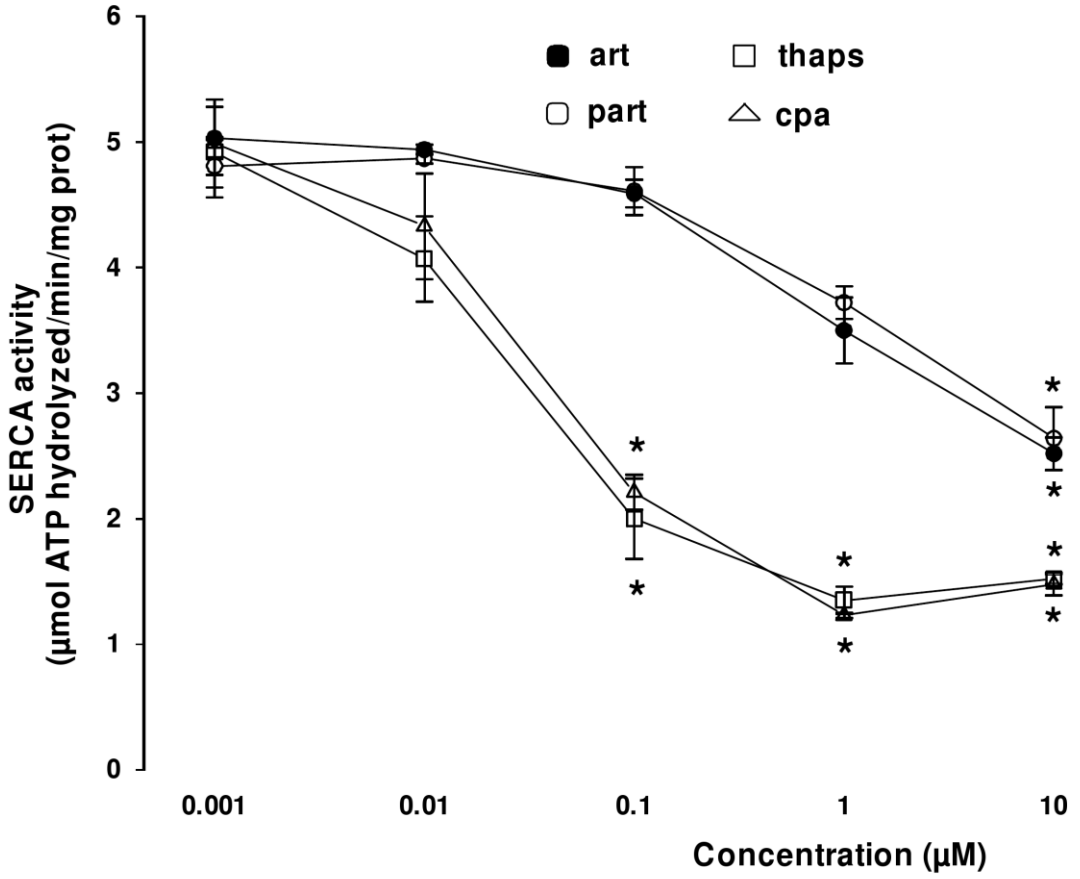
art
thaps
part
cpa
SERCA activity
(µmol ATP hydrolyzed/min/mg prot)
0
1
2
3
4
5
6
0.001
0.01
0.1
1
10
Concentration (µM)
*

Figure 2

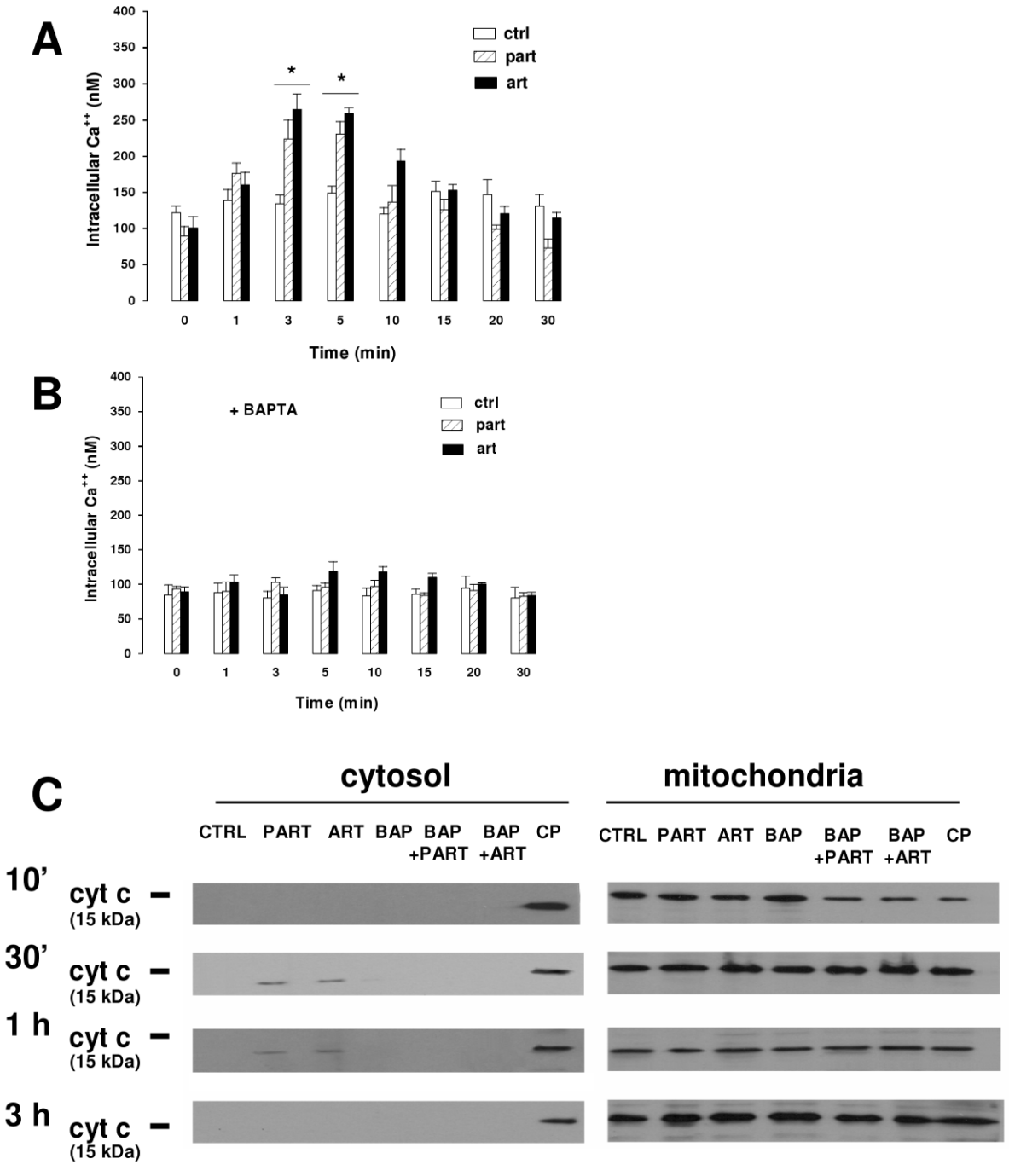
A
ctrl
part
art
Intracellular Ca++ (nM)
Time (min)
B
+ BAPTA
ctrl
part
art
Intracellular Ca++ (nM)
Time (min)
C
cytosol
mitochondria
CTRL PART ART BAP BAP +PART BAP +ART CP
CTRL PART ART BAP BAP +PART BAP +ART CP
10'
30'
1 h
3 h
cyt c
(15 kDa)

Figure 3

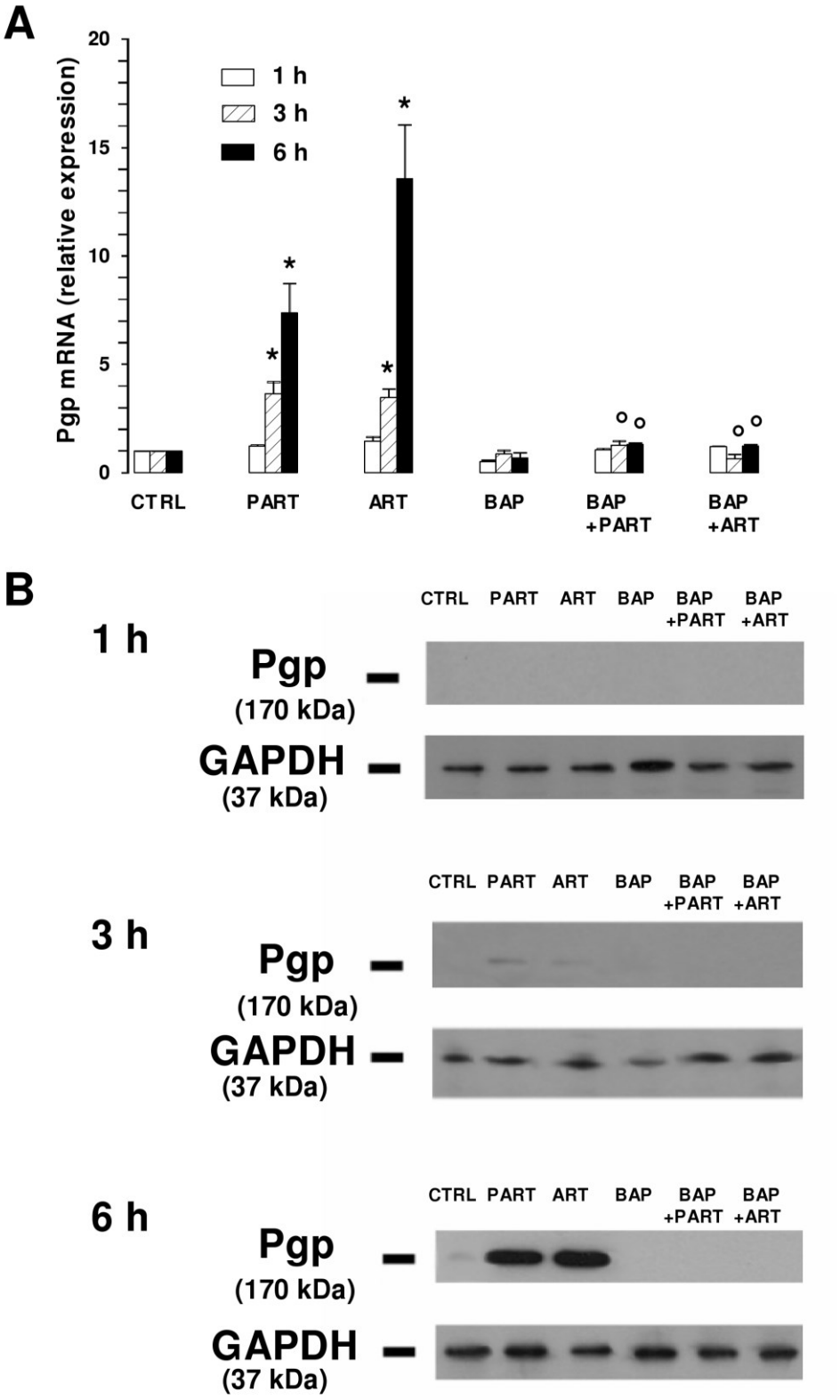
A
Pgp mRNA (relative expression)
20
15
10
5
0
1 h
3 h
6 h
*
*
*
*
°°
°°
CTRL
PART
ART
BAP
BAP +PART
BAP +ART
B
1 h
CTRL PART ART BAP BAP +PART BAP +ART
Pgp
(170 kDa)
GAPDH
(37 kDa)
3 h
CTRL PART ART BAP BAP +PART BAP +ART
Pgp
(170 kDa)
GAPDH
(37 kDa)
6 h
CTRL PART ART BAP BAP +PART BAP +ART
Pgp
(170 kDa)
GAPDH
(37 kDa)

Figure 4

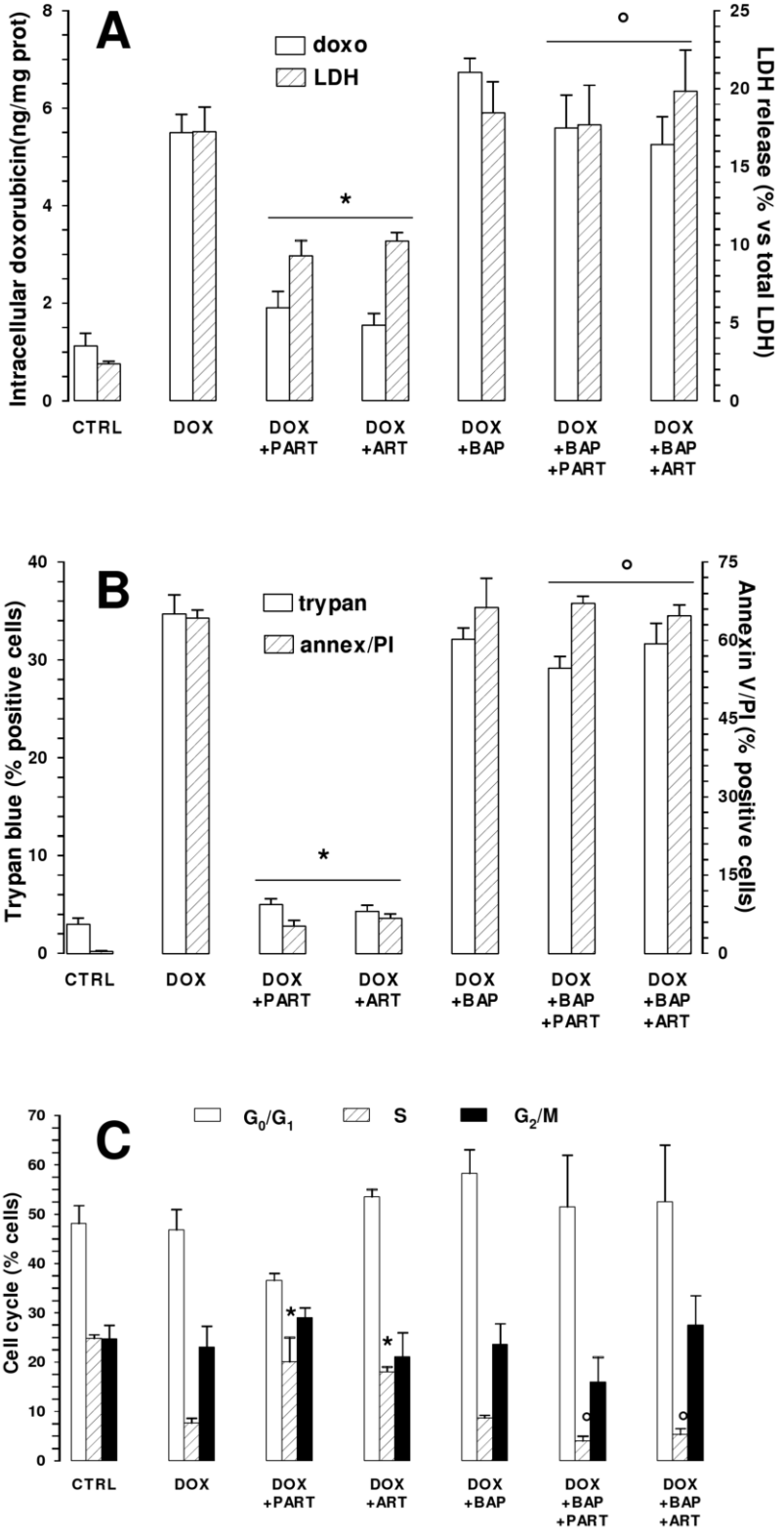
A
doxo
LDH
Intracellular doxorubicin(ng/mg prot)
LDH release (% vs total LDH)
CTRL
DOX
DOX +PART
DOX +ART
DOX +BAP
DOX +BAP +PART
DOX +BAP +ART
B
trypan
annex/PI
Trypan blue (% positive cells)
Annexin V/PI (% positive cells)
C
G0/G1
S
G2/M
Cell cycle (% cells)

Figure 5

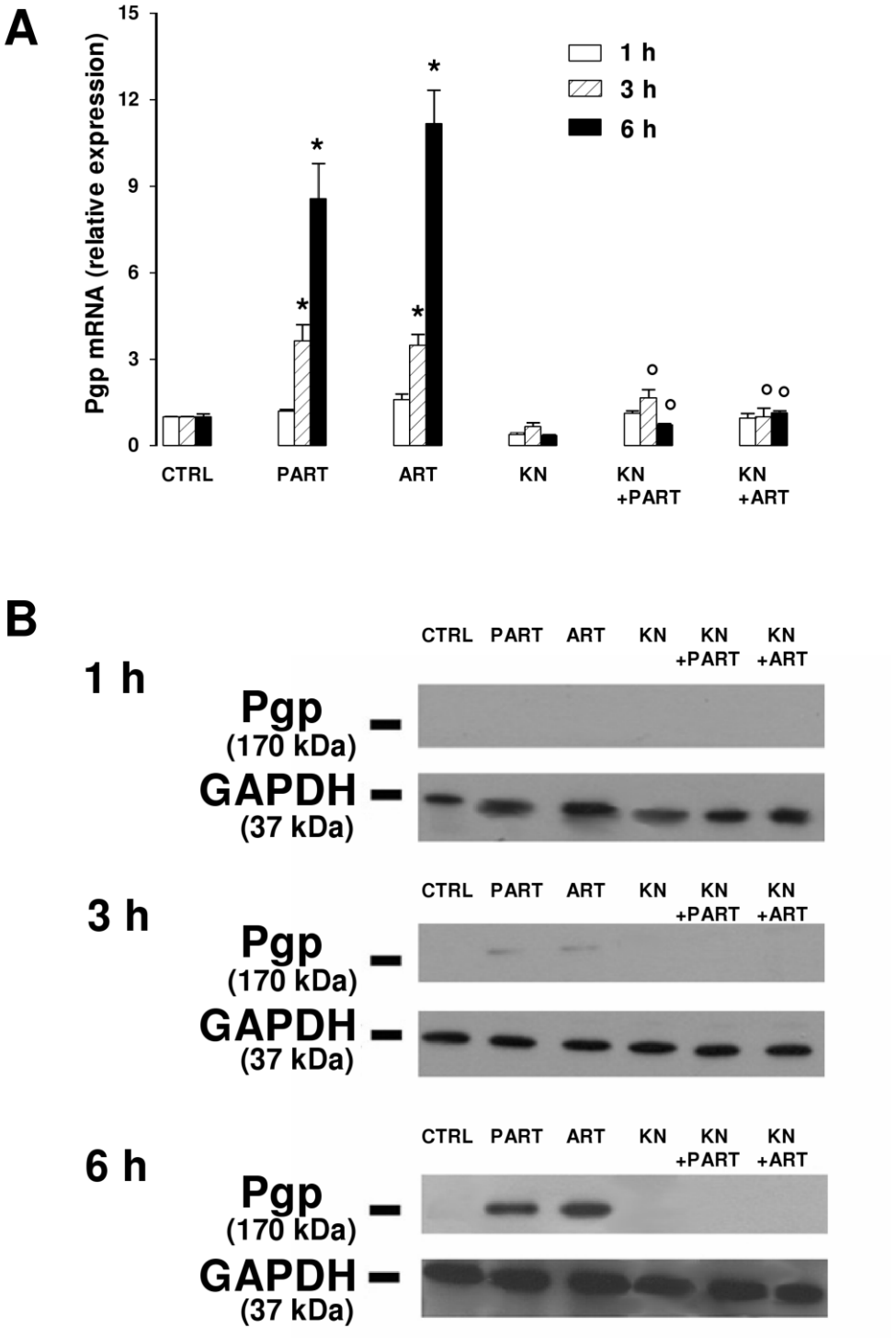
A
Pgp mRNA (relative expression)
15
12
9
6
3
0
1 h
3 h
6 h
CTRL
PART
ART
KN
KN +PART
KN +ART
B
1 h
3 h
6 h
CTRL PART ART KN KN +PART KN +ART
Pgp (170 kDa)
GAPDH (37 kDa)

Figure 6

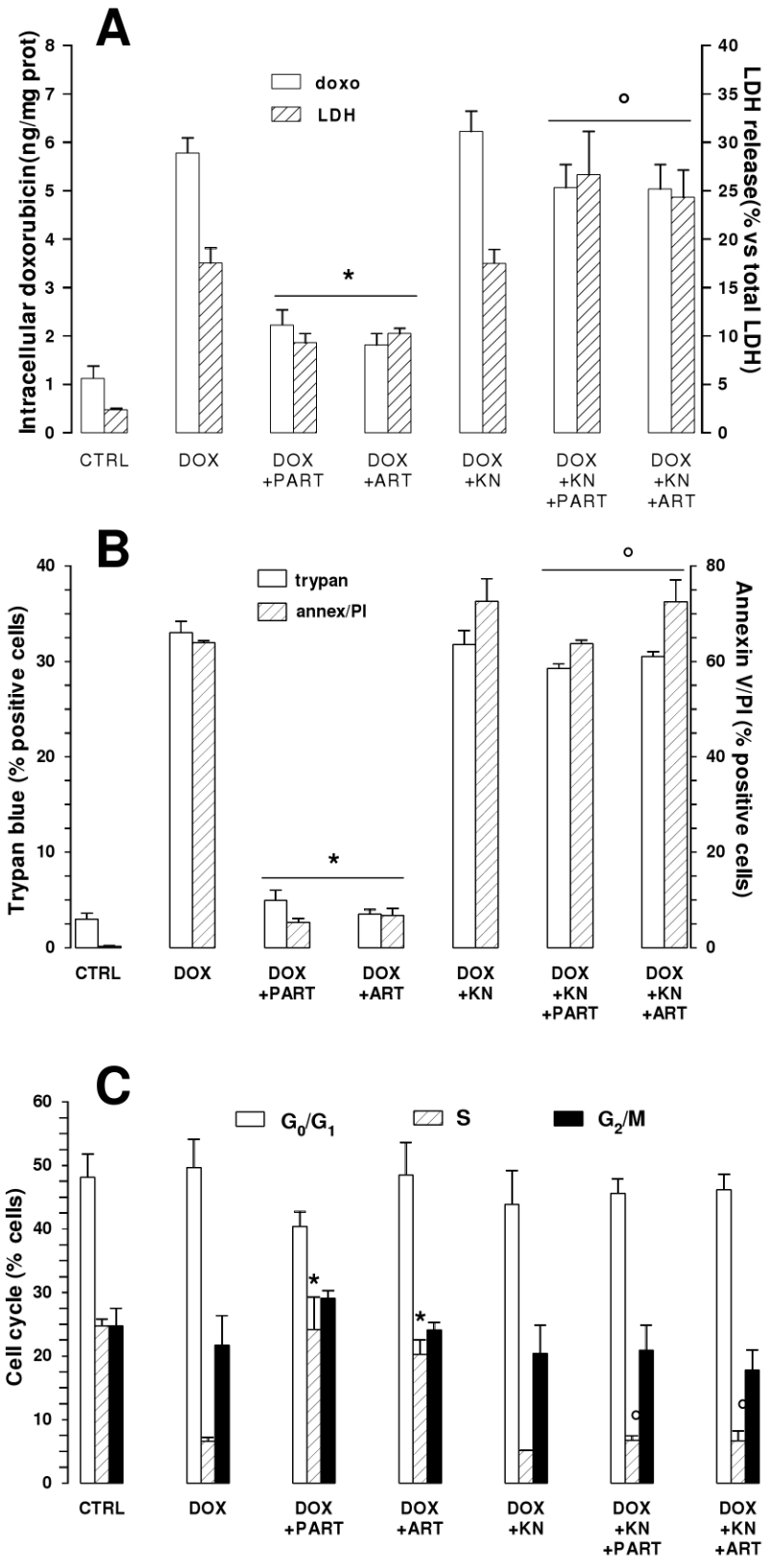
A
Intracellular doxorubicin(ng/mg prot)
LDH release(% vs total LDH)
doxo
LDH
*
°
CTRL
DOX
DOX +PART
DOX +ART
DOX +KN
DOX +KN +PART
DOX +KN +ART
B
Trypan blue (% positive cells)
Annexin V/PI (% positive cells)
trypan
annex/PI
*
°
CTRL
DOX
DOX +PART
DOX +ART
DOX +KN
DOX +KN +PART
DOX +KN +ART
C
Cell cycle (% cells)
G0/G1
S
G2/M
*
°
CTRL
DOX
DOX +PART
DOX +ART
DOX +KN
DOX +KN +PART
DOX +KN +ART

Figure 7

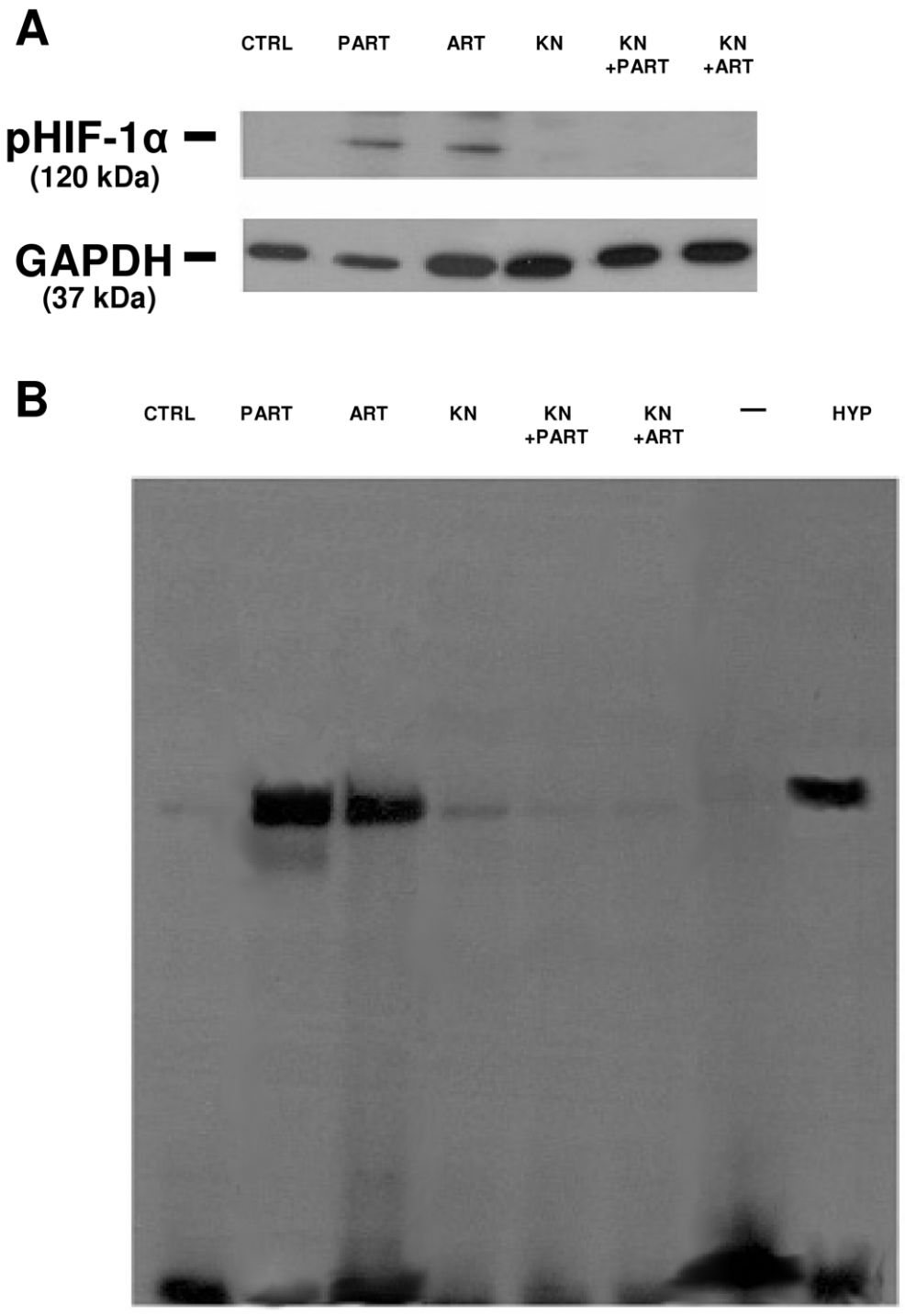
A
CTRL
PART
ART
KN
KN +PART
KN +ART
pHIF-1α
(120 kDa)
GAPDH
(37 kDa)
B
CTRL
PART
ART
KN
KN +PART
KN +ART
—
HYP

FIGURE LEGENDS OF SUPPLEMENTARY FILES

Figure S1. Densitometric analysis of Western blotting experiments. Panel A concerns the experimental conditions reported in Figure 3B, panel B is referred to the experimental conditions reported in Figure 5B of the manuscript. The band intensity, calculated by ImageJ Software (National Institutes of Health, Research Services Branch, Bethesda, MD, USA; available from http://rsb.info.nih.gov/ij/), and expressed as arbitrary units, is presented as mean ± SE (n =3). vs. *CTRL*: * $p < 0.05$; vs. *PART* or *ART* respectively: ° $p < 0.05$.

Figure S2. Effect of artemisinin, BAPTA-AM and KN93 on the apoptosis (panel A) and on the cell cycle arrest (panel B) induced by doxorubicin. HT29 cells were incubated for 6 h in the absence (*CTRL-DOXO*) or presence of 5 μM doxorubicin (*CTRL*) plus artemisinin (*ART*, 10 μM); when indicated, cells were pre-incubated for 1 h with BAPTA-AM (*BAP*, 10 μM) or co-incubated with KN93 (*KN*, 10 μM), alone or in different combinations. After these incubation times, cells were washed and let grow in fresh medium for 24 h, then stained with annexin V-FITC (*FL1-H*) and PI (*FL2-H*) as reported in the Materials and Methods section. To evaluate the cell cycle, cells were permeabilized with ethanol and incubated with PI as indicated under the Materials and Methods section. The dot plots and the histograms, obtained by the FACS analysis of cellular fluorescence, are representative of three experiments with similar results, obtained in HT29 cells incubated with artemisinin. The incubation with parthenolide produced superimposable results (see Figure 4B, 4C, 6B and 6C).

Figure S3. Effects of thapsigargin, parthenolide, artemisinin and cyclopiazonic acid on SERCA activity in LoVo, HepG2 and MCF-7 cells. 50 μg of purified SERCA protein were incubated in the absence or presence of thapsigargin (*thaps*, *open square*), parthenolide (*part*, *open circle*), artemisinin (*art*, *solid circle*), cyclopiazonic acid (*cpa*, *open diamond*), at different concentrations. SERCA activity was measured as described under the Materials and Methods section. Measurements were performed in duplicate and data are presented as means ± SE (n = 3). SERCA activity in control cells was 5.71 ± 0.28 μmol ATP hydrolyzed/min/mg prot for LoVo cells, 4.52 ±

0.19 μmol ATP hydrolyzed/min/mg prot for HepG2 cells, 4.89 ± 0.07 μmol ATP hydrolyzed/min/mg prot for MCF-7 cells (not shown in the figure). Significance vs *CTRL*: * $p < 0.001$ (LoVo); * $p < 0.005$ (HepG2); * $p < 0.001$ (MCF-7).

Figure S4. Effects of parthenolide and artemisinin on $[Ca^{++}]_i$ in LoVo (panel A and B), HepG2 (panel C and D), MCF-7 (panel E and F) cells. Cells were grown on sterile glass coverslips for 24 h, washed with PBS and incubated for 10 min in Hepes-Ca buffer containing 10 μM FURA-AM, in the absence (*CTRL, open bars*) or presence of parthenolide (*PART*, 10 μM, *hatched bars*) and artemisinin (*ART*, 10 μM, *solid bars*). When indicated, cells were pre-incubated for 1 h with 10 μM BAPTA-AM, then treated as reported above. Fluorescence was detected throughout the first 30 min, as described under Materials and Methods. Measurements were performed in duplicate and data are presented as means ± SE (n = 4). Significance of each drug vs *CTRL*: * $p < 0.005$ (LoVo); * $p < 0.005$ (HepG2); * $p < 0.05$ (MCF-7).

Figure S5. Effects of parthenolide and artemisinin on Pgp mRNA (panel A) and protein (panel B and C) in LoVo, HepG2 and MCF-7 cells. Cells were incubated for 3 h (panel A) or 6 h (panel B) in the absence (*CTRL*) or presence of parthenolide (*PART*, 10 μM) and artemisinin (*ART*, 10 μM). When indicated, cells were pre-incubated for 1 h with BAPTA-AM (*BAP*, 10 μM) or co-incubated with KN93 (*KN*, 10 μM). **A.** Total RNA was extracted, retro-transcribed and subjected to RT-PCR, performed as indicated under the Materials and Methods section. Measurements were performed in triplicate and data are presented as means ± SE (n = 3). Significance for LoVo cells: vs *CTRL*: * $p < 0.02$; vs *PART* or *ART* respectively: ° $p < 0.05$. Significance for HepG2 cells: vs *CTRL*: * $p < 0.005$; vs *PART* or *ART* respectively: ° $p < 0.05$. Significance for MCF-7 cells: vs *CTRL*: * $p < 0.05$; vs *PART* or *ART* respectively: ° $p < 0.05$. **B-C.** To detect the Pgp protein, cells were lysed and the whole cellular lysate was immunoprecipitated with an anti-Pgp polyclonal antibody. The immunoprecipitated proteins were subjected to Western blotting, using the same antibody (see

Materials and Methods). The expression of GAPDH, the product of an housekeeping gene, was used as a control of equal protein loading. The figure is representative of three experiments with similar results.

Figure S6. Effects of parthenolide and artemisinin on doxorubicin accumulation, cytotoxicity and viability in LoVo (panel A and B), HepG2 (panel C and D) and MCF-7 (panel E and F) cells. Cells were grown for 6 h in the absence (*CTRL*) or in the presence of doxorubicin (5 μM, *DOX*), together with either parthenolide (*PART*, 10 μM) or artemisinin (*ART*, 10 μM); when indicated, cells were pre-incubated for 1 h with BAPTA-AM (*BAP*, 10 μM) or co-incubated with KN93 (*KN*, 10 μM), alone or in different combinations. Doxorubicin intracellular accumulation, release of LDH activity in the culture supernatant, positivity of Trypan blue and FACS analysis for annexin V and PI-positive cells were measured as described under Materials and Methods. Measurements were performed in duplicate and data are presented as means $\pm$ SE (n = 3). The significance of *DOX* vs *CTRL* was $p < 0.05$ for all the cell lines (not reported in the figure). Significance for LoVo cells: vs *DOX*: * $p < 0.002$; vs DOX+*PART* or DOX+*ART* respectively: $^{\circ}$ $p < 0.002$. Significance for HepG2 cells: vs *DOX*: * $p < 0.05$; vs DOX+*PART* or DOX+*ART* respectively: $^{\circ}$ $p < 0.02$. Significance for MCF-7 cells: vs *DOX*: * $p < 0.005$; vs DOX+*PART* or DOX+*ART* respectively: $^{\circ}$ $p < 0.005$.

Figure S7. Effects of parthenolide and artemisinin on the cell cycle arrest induced by doxorubicin in LoVo, HepG2 and MCF-7 cells. Cells were grown for 6 h in the absence (*CTRL*) or presence of doxorubicin (5 μM, *DOX*), together with either parthenolide (*PART*, 10 μM) or artemisinin (*ART*, 10 μM); when indicated, cells were pre-incubated for 1 h with BAPTA-AM (*BAP*, 10 μM) or co-incubated with KN93 (*KN*, 10 μM), alone or in combination. After this incubation time, cells were washed and let grow for 24 h in fresh medium, then they were permeabilized in ethanol and incubated with PI as indicated in the Materials and Methods section. Cell cycle analysis of G_0/G_1 phase (*open bars*), S phase (*hatched bars*) and G_2/M phase (*solid bars*) was obtained by a

FACSCalibur system using the Cell Quest software. Measurements were performed in duplicate and data are presented as means ± SE (n = 2). The significance of *DOX* vs *CTRL* was $p < 0.05$ for all the cell lines (not reported in the figure). Significance for LoVo cells: vs *DOX*: * $p < 0.05$; vs DOX+*PART* or DOX+*ART* respectively: ° $p < 0.05$. Significance for HepG2 cells: vs *DOX*: * $p < 0.05$; vs DOX+*PART* or DOX+*ART* respectively: ° $p < 0.05$. Significance for MCF-7 cells: vs *DOX*: * $p < 0.05$; vs DOX+*PART* or DOX+*ART* respectively: ° $p < 0.05$.

Figure S8. Effect of parthenolide, artemisinin and KN93 on HIF-1α phosphorylation (pHIF-1α) in LoVo cells, HepG2 cells and MCF-7 cells. Cells were incubated for 3 h in the absence (*CTRL*) or presence of either parthenolide (*PART*, 10 μM) or artemisinin (*ART*, 10 μM), alone or together with KN93 (*KN*, 10 μM). Cell lysates were incubated with an anti-HIF-1α antibody, subsequently the immunoprecipitated proteins were separated by SDS-PAGE and probed with an anti-phosphoserine antibody as described under the Materials and Methods section. The expression of GAPDH was used as a control of equal protein loading. The figure is representative of three experiments with similar results.

Figure S1

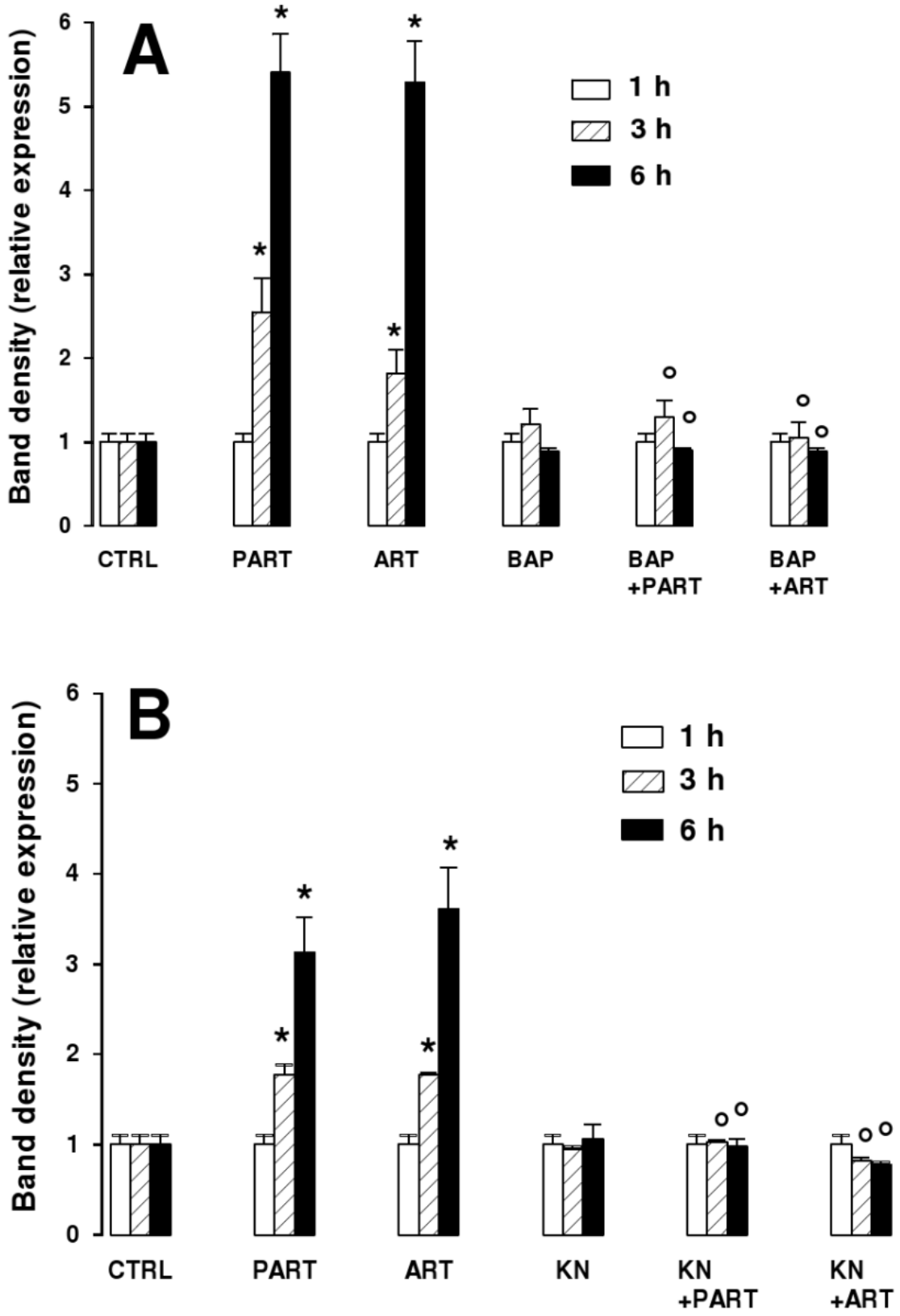
A
Band density (relative expression)
0
1
2
3
4
5
6
1 h
3 h
6 h
CTRL
PART
ART
BAP
BAP +PART
BAP +ART
B
Band density (relative expression)
0
1
2
3
4
5
6
1 h
3 h
6 h
CTRL
PART
ART
KN
KN +PART
KN +ART

Figure S2

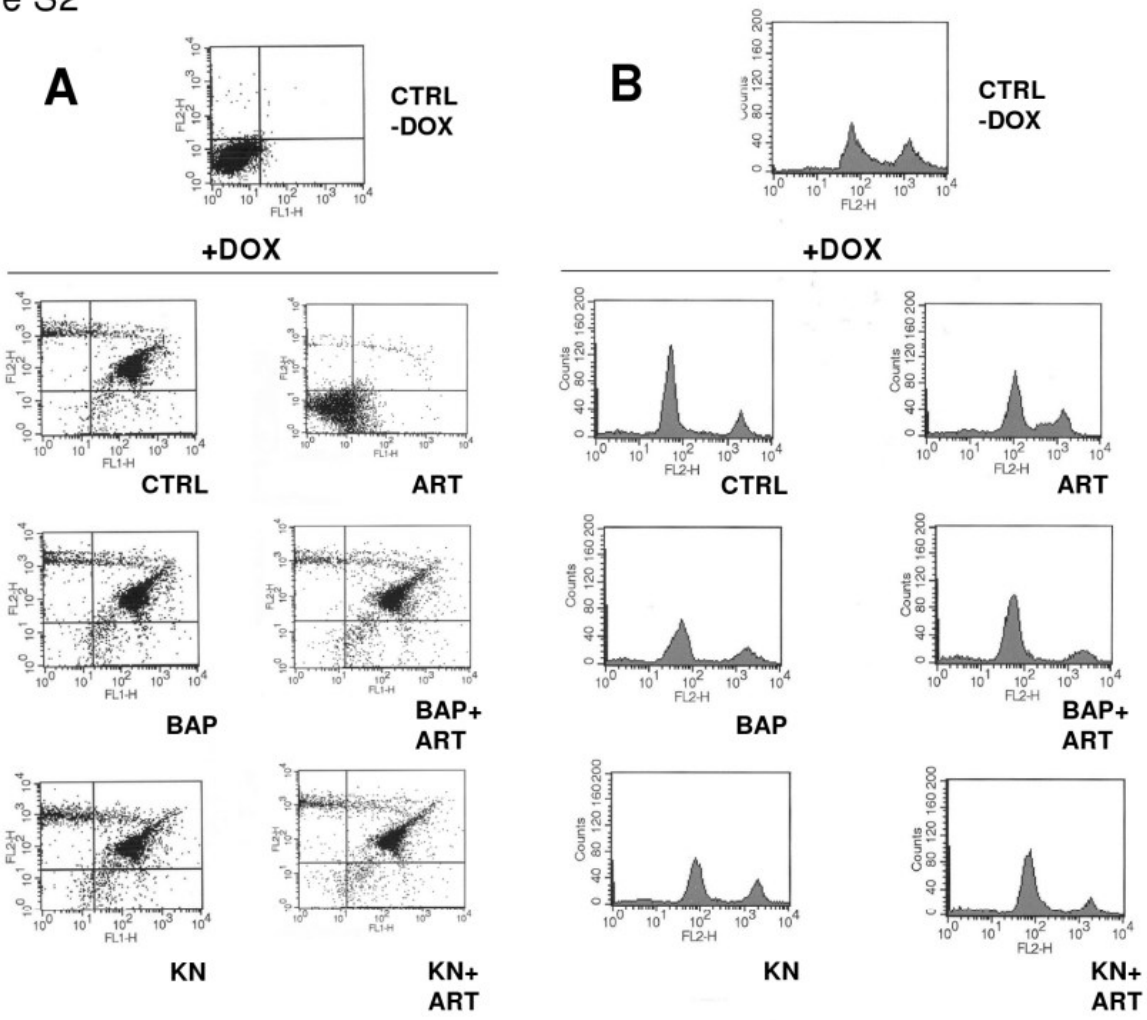

Figure S3

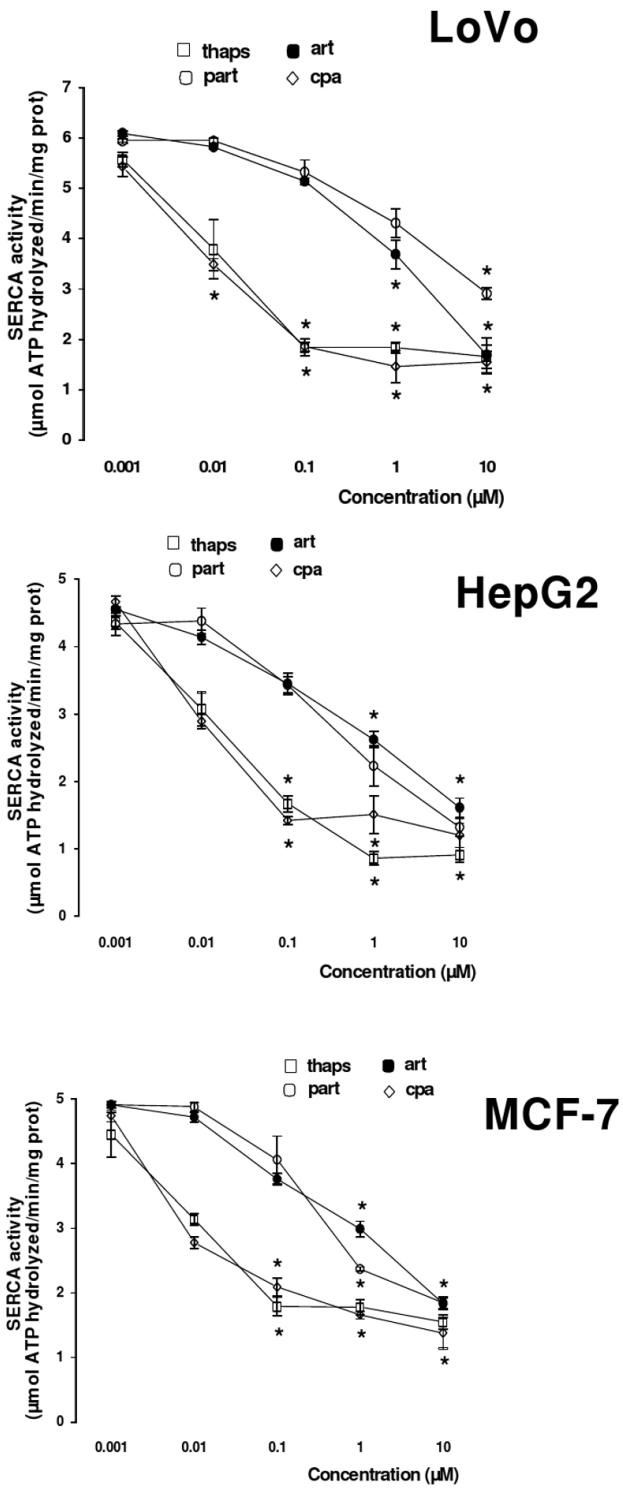
LoVo
thaps
art
part
cpa
SERCA activity
(µmol ATP hydrolyzed/min/mg prot)
0
1
2
3
4
5
6
7
0.001
0.01
0.1
1
10
Concentration (µM)
HepG2
thaps
art
part
cpa
SERCA activity
(µmol ATP hydrolyzed/min/mg prot)
0
1
2
3
4
5
0.001
0.01
0.1
1
10
Concentration (µM)
MCF-7
thaps
art
part
cpa
SERCA activity
(µmol ATP hydrolyzed/min/mg prot)
0
1
2
3
4
5
0.001
0.01
0.1
1
10
Concentration (µM)

Figure S4

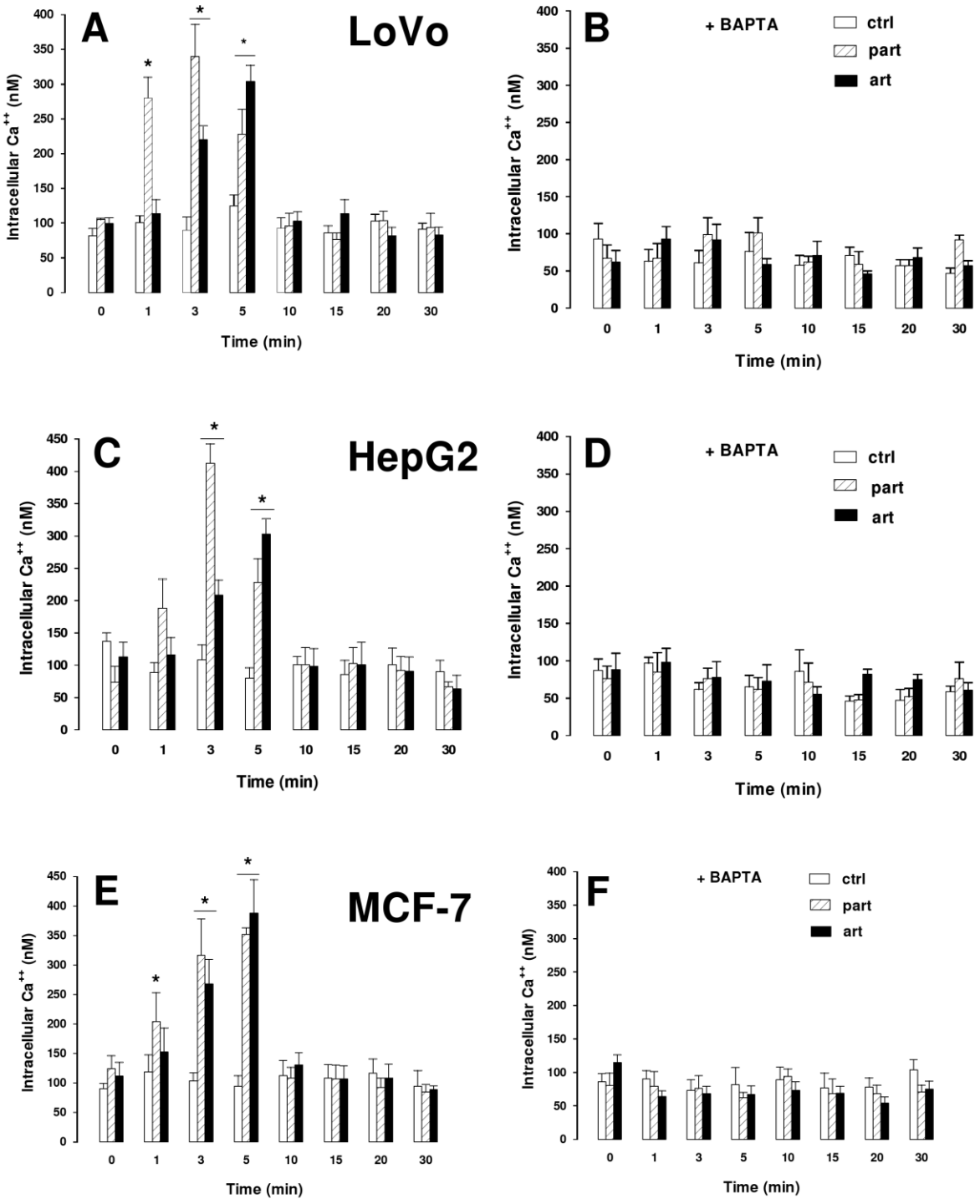
A
LoVo
B
+ BAPTA
ctrl
part
art
C
HepG2
D
+ BAPTA
ctrl
part
art
E
MCF-7
F
+ BAPTA
ctrl
part
art
Intracellular Ca++ (nM)
Time (min)
0
1
3
5
10
15
20
30

Figure S5

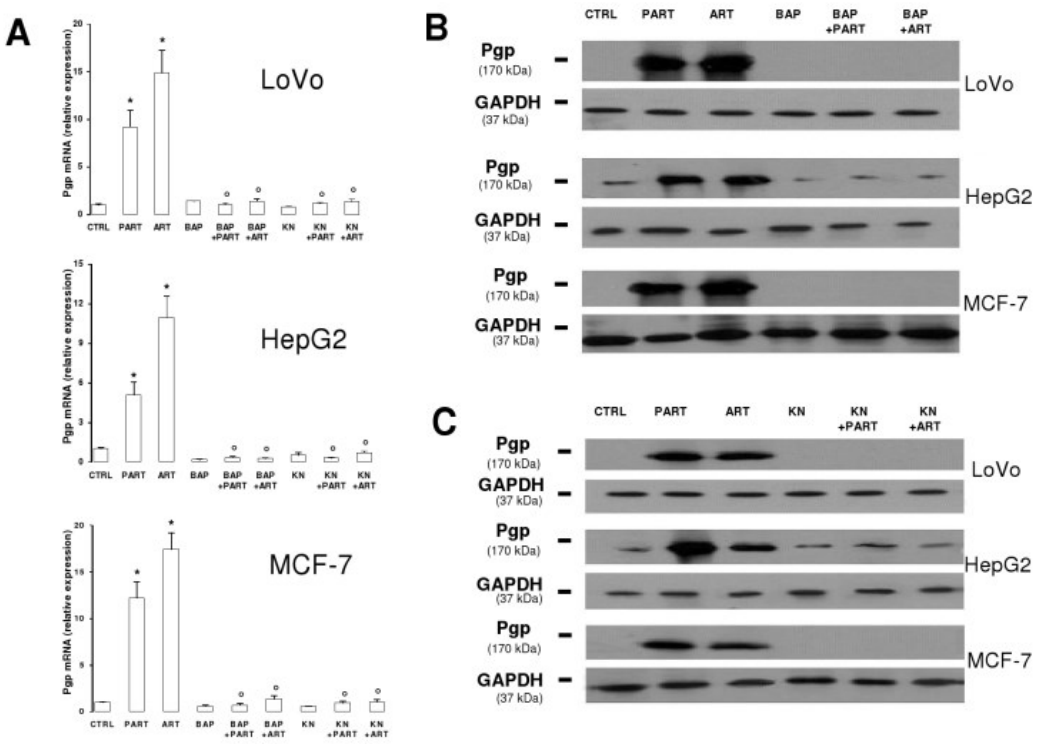
A
LoVo
HepG2
MCF-7
Pgp mRNA (relative expression)
CTRL
PART
ART
BAP
BAP +PART
BAP +ART
KN
KN +PART
KN +ART
B
Pgp (170 kDa)
GAPDH (37 kDa)
LoVo
HepG2
MCF-7
C

Figure S6

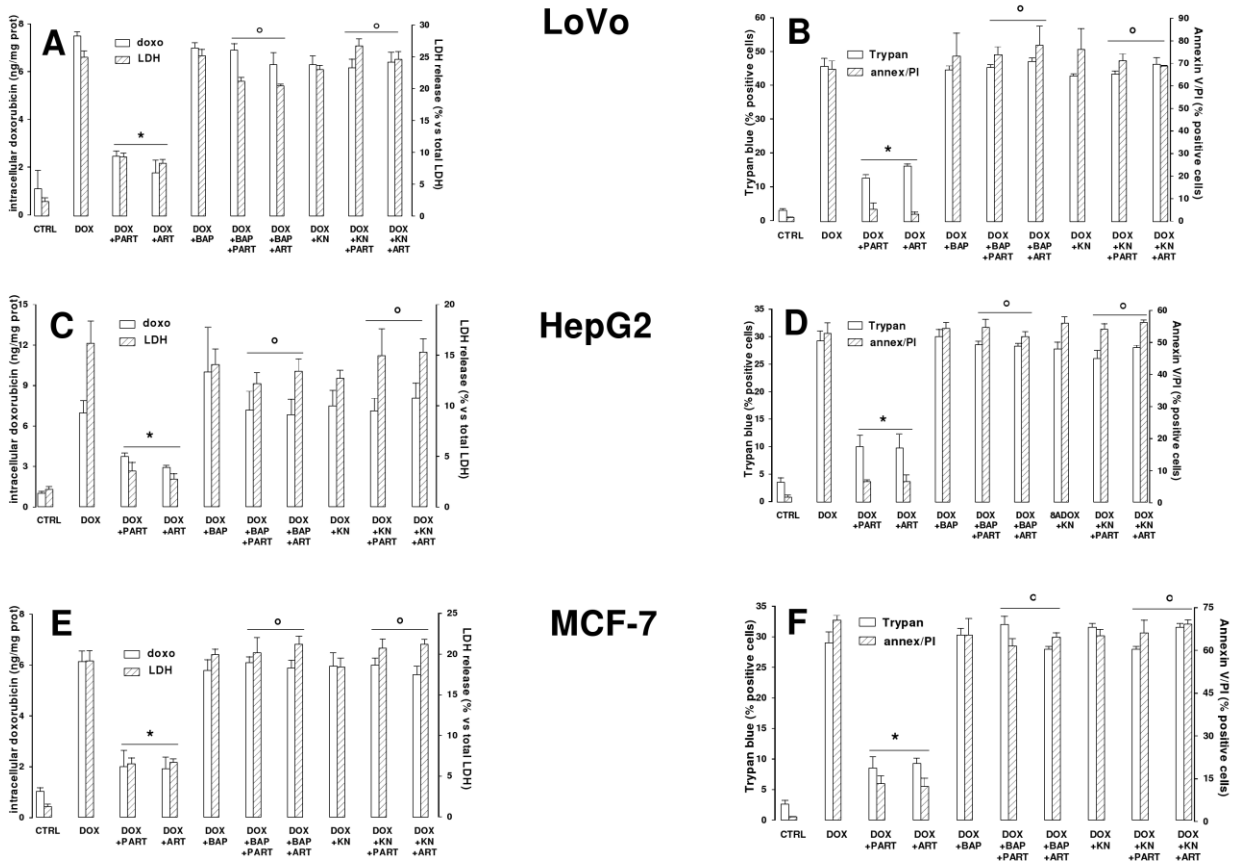
LoVo
HepG2
MCF-7
A
B
C
D
E
F
doxo
LDH
Trypan
annex/PI
intracellular doxorubicin (ng/mg prot)
LDH release (% vs total LDH)
Trypan blue (% positive cells)
Annexin V/PI (% positive cells)
CTRL
DOX
DOX +PART
DOX +ART
DOX +BAP
DOX +BAP +PART
DOX +BAP +ART
DOX +KN
DOX +KN +PART
DOX +KN +ART
6ADOX +KN

Figure S7

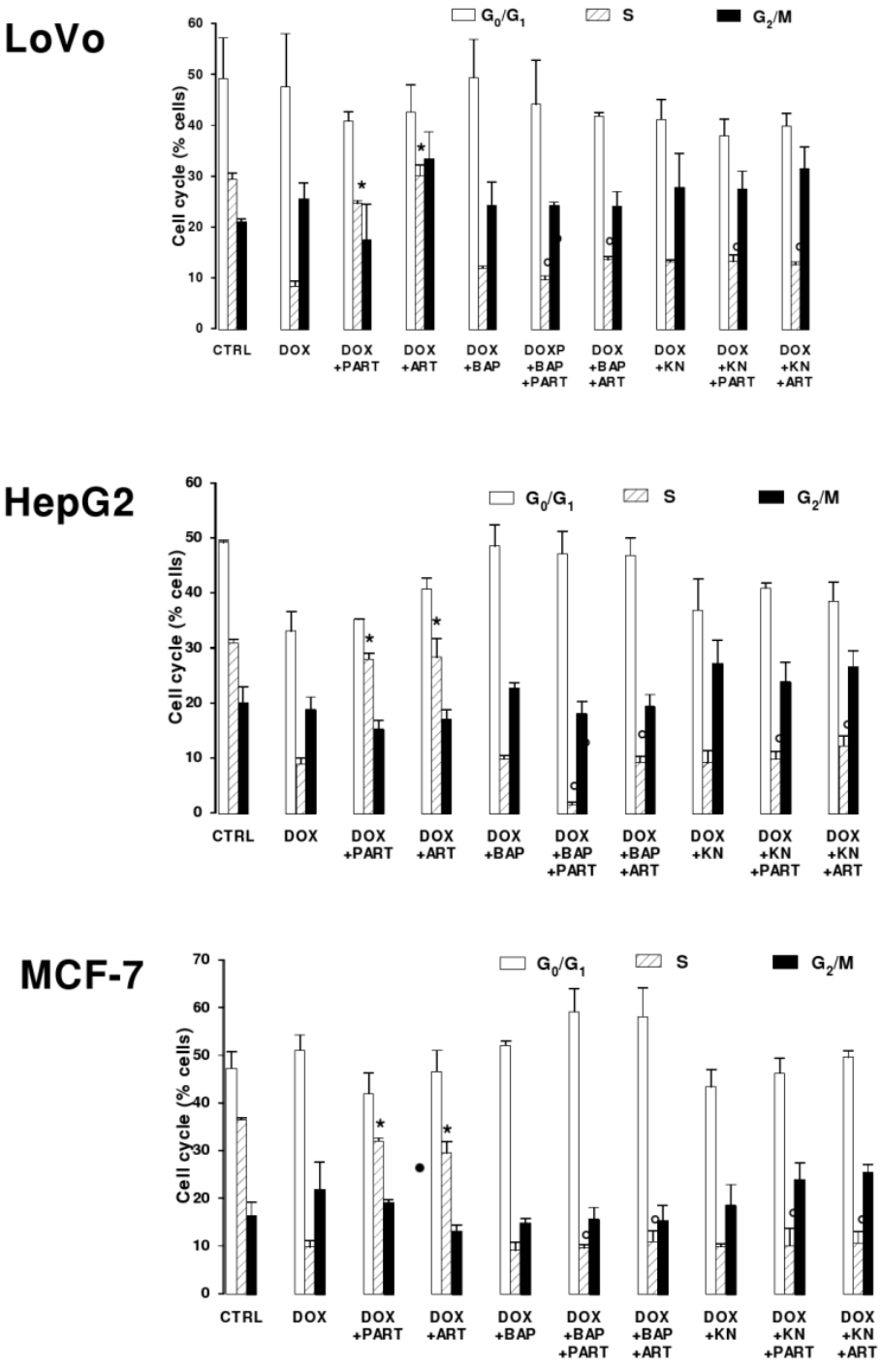
LoVo
HepG2
MCF-7
G0/G1
S
G2/M
Cell cycle (% cells)
CTRL
DOX
DOX +PART
DOX +ART
DOX +BAP
DOXP +BAP +PART
DOX +BAP +ART
DOX +KN
DOX +KN +PART
DOX +KN +ART

Figure S8

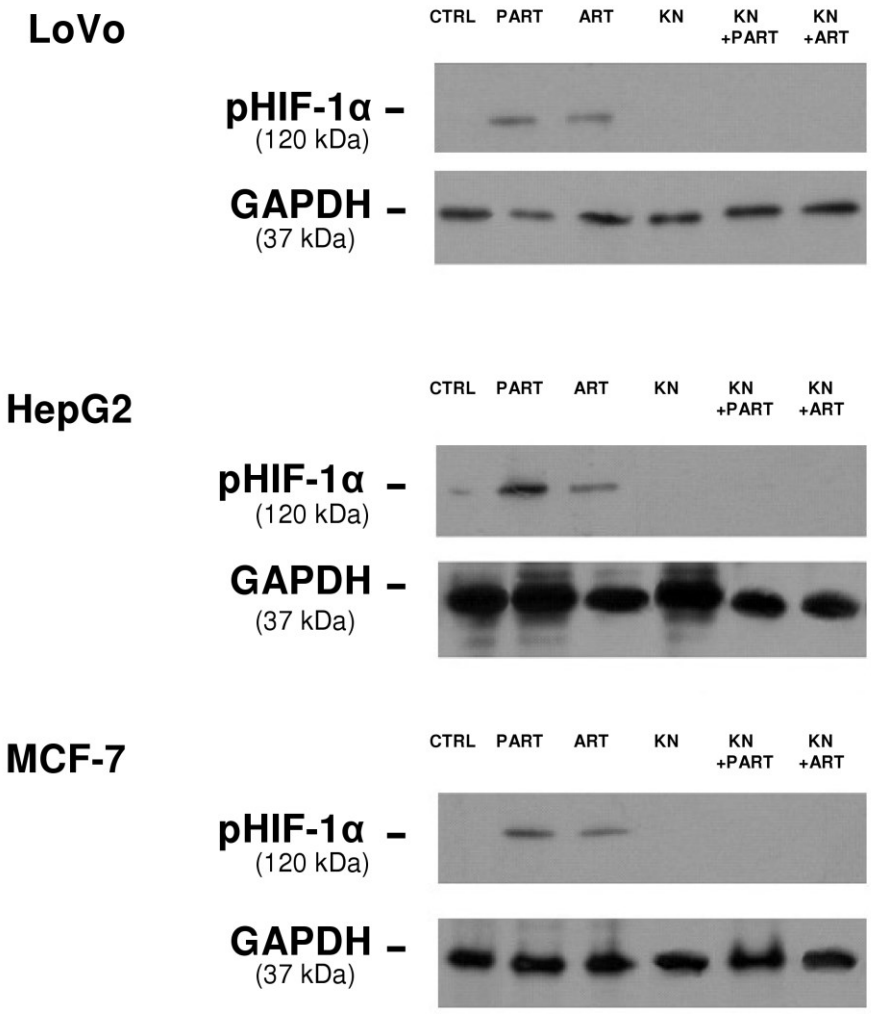
LoVo
CTRL
PART
ART
KN
KN +PART
KN +ART
pHIF-1α –
(120 kDa)
GAPDH –
(37 kDa)
HepG2
CTRL
PART
ART
KN
KN +PART
KN +ART
pHIF-1α –
(120 kDa)
GAPDH –
(37 kDa)
MCF-7
CTRL
PART
ART
KN
KN +PART
KN +ART
pHIF-1α –
(120 kDa)
GAPDH –
(37 kDa)